

## ORIGINAL ARTICLE

# Foxg1 Antagonizes Neocortical Stem Cell Progression to Astrogenesis

Carmen Falcone<sup>1,2</sup>, Manuela Santo<sup>1</sup>, Gabriele Liuzzi<sup>1</sup>, Noemi Cannizzaro<sup>1</sup>, Clara Grudina<sup>1,3</sup>, Erica Valencic<sup>4</sup>, Luca Peruzzotti-Jametti<sup>5</sup>, Stefano Pluchino<sup>5</sup> and Antonello Mallamaci<sup>1</sup>

<sup>1</sup>Laboratory of Cerebral Cortex Development, Neuroscience Area, SISSA, 34136 Trieste, Italy, <sup>2</sup>Current address: Institute for Pediatric Regenerative Medicine and Shriners Hospitals for Children Northern California, UC Davis, Sacramento, CA 95817, USA, <sup>3</sup>Current address: Institut Pasteur, 25-28 Rue du Dr Roux, 75015 Paris, France, <sup>4</sup>Department of Diagnostics, Institute for Maternal and Child Health, IRCCS Burlo Garofolo, 34137 Trieste, Italy and <sup>5</sup>Dept of Clinical Neurosciences, University of Cambridge, Clifford Allbutt Building – Cambridge Biosciences Campus, Hills Road, CB2 0HA Cambridge, UK

Address correspondence to Antonello Mallamaci, Via Bonomea, 265-34136 Trieste, Italy. Email: amallama@sissa.it

## Abstract

Neocortical astrogenesis follows neuronogenesis and precedes oligogenesis. Among key factors dictating its temporal articulation, there are progression rates of pallial stem cells (SCs) towards astroglial lineages as well as activation rates of astrocyte differentiation programs in response to extrinsic gliogenic cues. In this study, we showed that high Foxg1 SC expression antagonizes astrocyte generation, while stimulating SC self-renewal and committing SCs to neuronogenesis. We found that mechanisms underlying this activity are mainly cell autonomous and highly pleiotropic. They include a concerted downregulation of 4 key effectors channeling neural SCs to astroglial fates, as well as defective activation of core molecular machineries implementing astroglial differentiation programs. Next, we found that SC Foxg1 levels specifically decline during the neuronogenic-to-gliogenic transition, pointing to a pivotal Foxg1 role in temporal modulation of astrogenesis. Finally, we showed that Foxg1 inhibits astrogenesis from human neocortical precursors, suggesting that this is an evolutionarily ancient trait.

**Key words:** astrogenesis, commitment, differentiation, Foxg1, NSC

Neocortical astrocytes are generated according to a peculiar, spatiotemporal, and clonal pattern. They originate from neural precursors located in neopallial periventricular layers (Gorski et al. 2002; Tsai et al. 2012), largely via committed progenitors. Still intermitotic, these progenitors migrate towards more marginal layers, where they locally proliferate and give rise to mature differentiated progenies (Ge et al. 2012; Magavi et al. 2012). Astrogenesis initiates at low levels at mid-neuronogenic stages and peaks up after neuronogenesis completion (Okano and Temple 2009). Clonal trees originating from isolated, early

pallial stem cells reveal the early occurrence of neuronal progenitors and later appearance of glia- and astroglia-committed precursors (Qian et al. 2000). All these precursors are detectable in vivo along a largely consistent temporal progression (Costa et al. 2009).

Among processes dictating the ultimate neocortical astroglial output there is the transition from early neural stem cells (NSCs) to astrocyte-committed progenitors, namely a key developmental step requiring an accurate molecular control. This control is exerted by a large set of genes, most of which have

been implicated in a dense and intricate functional network (Mallamaci 2013; Kanski et al. 2014; Sloan and Barres 2014; Takouda et al. 2017). A small group of transcription factors, including CoupTf1/II, Zbtb20, Sox9, and Nfia, promote the astrogenesis onset, partly by changing the epigenetic state of astroglial genes (Naka et al. 2008; Namihira et al. 2009; Kang et al. 2012; Nagao et al. 2016). Once chromatin of genes active in astroglia gets permissive, then its transcription rate results from the interaction among dedicated signaling pathways, impinging on astroglial promoters. Some of them inhibit astroglial gene transcription (e.g., Nrg1/ErbB4<sup>CD</sup>-NCoR (Hermanson et al. 2002; Sardi et al. 2006; Schlessinger and Lemmon 2006; Miller and Gauthier 2007)), some others promote it (e.g., IL6/Jak2/Stat1,3) (Derouet et al. 2004; Barnabé-Heider et al. 2005; He et al. 2005), Bmp/Smad1,5,8 (Nakashima 1999; Sun et al. 2001), Dll1/Notch1<sup>CD</sup> (Ge et al. 2002; Kamakura et al. 2004).

We previously found that pallial NSC-restricted overexpression of *Foxg1*, an ancient transcription factor controlling telencephalic specification (Hanashima et al. 2007), subpallial/pallial fate (Manuel et al. 2010; Mariani et al. 2015; Patriarchi et al. 2016), hippocampal programs (Muzio and Mallamaci 2005), and neuronogenesis progression (Miyoshi and Fishell 2012; Toma et al. 2014; Chiola et al. 2019), leads to a substantial decrease of astrocyte generation (Brancaccio et al. 2010). However, we demonstrated the occurrence of this phenomenon only in a murine, heterochronic in vitro system, we did not address its physiological relevance and, last, we did not focus on molecular mechanisms underlying it (Brancaccio et al. 2010).

In this study we showed that *Foxg1* overexpression within neocortical stem cells commits these cells to neuronogenesis rather than astrogenesis, in vivo as well as in vitro, both in mouse and human. Interestingly, we found that *Foxg1* inhibition of astrogenesis stems from variegated mechanisms. These include a direct trans-repression of genes biasing NSCs to astroglial fates, as well as an articulated impact on key pathways which modulate astroglial gene transcription, resulting into a robust dampening of it. Finally, we provided evidence that *Foxg1* levels decline, while neocortical NSCs move from neuronogenesis to gliogenesis.

These findings point to an evolutionarily conserved, pivotal role of *Foxg1* in fine temporal regulation of astrogenesis. They also suggest that neurological symptoms observed in syndromes with altered *Foxg1* allele dosage (Guerrini and Parrini 2012) might be partially caused by an unbalanced astrocyte generation.

## Materials and Methods

### Animal Handling and Embryo Dissection

Animal handling and subsequent procedures were in accordance with European and Italian laws (European Parliament and Council Directive of 22 September 2010 [2010/63/EU]; Italian Government Decree of 04 March 2014, no. 26). Experimental protocols were approved by SISSA OpBA (Institutional SISSA Committee for Animal Care) and authorized by the Italian Ministry of Health (Auth. No. 1231/2015-PR of 25 November 2015).

Wild type (strain CD1, purchased from Envigo, Italy) and *Foxg1*<sup>+/-</sup> strain (Hébert and McConnell 2000) were maintained at the SISSA animal facility. Embryos were staged by timed breeding and vaginal plug inspection. Pregnant females were sacrificed by cervical dislocation. Embryonic cortices were dissected out in cold 1X-phosphate buffered saline (PBS), under sterile conditions.

### Derivation of Human Neocortical Precursor Line

NPCs were derived from the cerebral cortex of a single 10.2 post conception week (PCW) human fetus, collected from routine termination of pregnancies under full ethical approval in line with Department of Health guidelines (LREC 96/085;96/085—In vitro study of postmortem human fetal neural tissue, blood and haematopoietic organs, approved by Cambridge Central Ethics Committee). Cells were grown and expanded in a chemically defined, serum-free medium in the presence of Fibroblast Growth Factor 2 (Fgf2) and Epidermal Growth Factor (Egf) (10 and 20 ng/mL, respectively) and routinely assessed for multipotency, as described (Pluchino et al. 2009).

Derivation of human neocortical precursor line, Lentiviral Vectors Packaging and Titration, Engineering cells for in vivo transplantation, in vivo neural precursor cell transplantation, histology brain sample preparation, cortical cultures, for differentiation assays, and mRNA profiling, immunofluorescence analysis, analytical cytofluorimetry: cell preparation and analysis, preparative cytofluorimetry: cell preparation and sorting, RNA profiling: qRT-PCR, ChIP-qPCR.

They were performed according to standard protocols. Temporal articulation of protocols and molecular tools for their implementation are illustrated in dedicated figure panels (Figs 1–6 and S8). Full protocol details, including lists of lentiviruses, PCR oligo sequences and antibodies employed, are provided in Supplementary Material.

## Results

### *Foxg1* Overexpression in Murine Neocortical NSCs Antagonizes Astrogenesis

Previous investigations in our lab gave evidence for a reduction of the astroglial output following *Foxg1* overexpression in NSCs (Brancaccio et al. 2010). However, this phenomenon was only documented in vitro, as well as in a temporal frame delayed as compared with the standard astroglial schedule (Okano and Temple 2009). Based on these findings, we hypothesized that *Foxg1* might also control the physiological, timed progression of neocortical NSCs towards glial fates. To test this hypothesis, we decided to assess if *Foxg1* overexpression impacts the in vivo astroglial output of genetically manipulated NSCs transplanted into wild type recipient brains, according to a developmentally plausible schedule. For this purpose, we engineered dissociated E12.5 corticocerebral precursors for conditional, TetON-driven *Foxg1* overexpression, under the control of aNestin gene-derivative promoter (pNes) selectively firing in NSCs (Brancaccio et al. 2010). We acutely activated the transgene via doxycyclin administration and we maintained cells in a proliferative medium for 7 days. Then, we transplanted cells into the parietal corticocerebral parenchyma of P0 isochronic mouse pups. Specifically, we injected a 1:1 mix of cells, made alternatively gain-of-function (GOF) for *Foxg1* or a control, and labeled with EGFP and mCherry, respectively. Four days later, we sacrificed the pups and scored their brains for the astroglial outputs of the 2 different, transplanted precursor types (Fig. 1A,D). For this purpose, we took advantage of S100b, a Ca<sup>2+</sup>-binding protein shared by ependyma and glial lineages, mainly expressed by astroglial cells of perinatal neocortical tissue (Deloulme et al. 2004; Raponi et al. 2007; Falcone et al. 2015). We found that, compared with controls, S100b<sup>+</sup> derivatives of *Foxg1*-GOF cells were reduced by  $19.25 \pm 6.94\%$  ( $P < 9.60 \times 10^{-6}$ ,  $n = 8,8$ , paired t-test) (Fig. 1E, right and Fig. S1B). As *Foxg1* also promotes NSCs self-renewal (Brancaccio et al., 2010),

we reasoned that this might lead us to underestimate the actual impact of *Foxg1* overexpression on the NSC astrogenic bias. Therefore, to compensate for such an effect, first, we evaluated the frequency of Nestin<sup>+</sup> NSCs within sister cell preparations, engineered like the transplanted ones (but not labeled by EGFP or mCherry) and kept in proliferative medium for 7 days (Fig. 1A,D). Then, we normalized the in vivo astroglial output of transplanted cells against such frequency. We found that *Foxg1* overexpression induced a 2.5-folds increase of Nestin<sup>+</sup> cells ( $+149.76 \pm 6.34\%$ ,  $P < 4.55 \times 10^{-7}$ ,  $n = 3,3$ ) (Fig. 1E, left and Fig. S1A), meaning that the average, NSCs-normalized S100 $\beta$ <sup>+</sup> astrocytic output was decreased by as much as 67.67%.

To corroborate these results, we performed a specular loss-of-function assay, employing neural precursors alternatively engineered by an  $\alpha$ *Foxg1*-shRNA-expressing-LV or a control (Fig. 1B,D). Here we expected an enlargement of the astroglial output. Consequently, to increase the sensitivity of the assay, we interrogated E12.5 precursor derivatives kept in vitro for only 4 days being therefore further from the astrogenic peak. Specifically, we cotransplanted these cells as 1:1 mixes into heterochronic P0 pups and we assessed their final glial output at P4. The S100 $\beta$ <sup>+</sup> cells frequency did not change upon *Foxg1* manipulation ( $n = 4,4$ ) (Fig. 1F, right and Fig. S1D). However, on the day of transplantation, the frequency of Nestin<sup>+</sup> cells was decreased by  $32.14 \pm 3.26\%$  ( $P < 1.12 \times 10^{-3}$ ,  $n = 3,3$ ) in  $\alpha$ *Foxg1*-shRNA samples compared with controls (Fig. 1F, left and Fig. S1C). This means that  $\alpha$ *Foxg1*-shRNA manipulation upregulated the average, NSC-normalized astrogenic output by 39.75%.

To further validate these results, we repeated our GOF assay restricting the manipulation of *Foxg1* NSC levels to the in vivo environment. To this aim, we kept dissociated E11.5 corticocerebral precursors, made acutely *Foxg1*-GOF under pNes/TetON control, for 3 days in a doxy-free proliferative medium. Then, we transplanted a 1:1 mix of these cells (EGFP-labeled) and their controls (mCherry-labeled) into the lateral ventricle of E14.5 isochronic mouse embryos. Last, we activated *Foxg1* and control transgenes via oral doxycyclin administration to pregnant females. We allowed the embryos to be born, we sacrificed the pups at P4, and we evaluated the astroglial outputs of the 2 different, transplanted precursor types (Fig. 1C,D). Similarly to the first *Foxg1*-GOF assay, we found that S100 $\beta$ <sup>+</sup> derivatives of *Foxg1*-GOF precursors were robustly reduced compared with controls ( $-24.08 \pm 11.03\%$ ,  $P < 0.01$ ,  $n = 4,4$ , paired t-test) (Figs 1G and S1E), so definitively pointing to a genuine *Foxg1* antiastrogenic activity.

To model molecular mechanisms underlying this activity, we considered to investigate them in dissociated neural cultures. To confirm the feasibility of this approach, we first verified if the outcome of *Foxg1* manipulation could be fully replicated in these cultures, within a biologically acceptable temporal framework. For this purpose, we engineered dissociated E12.5 corticocerebral precursors for conditional *Foxg1* overexpression as described above for transplantation assays, we maintained these cells in a proliferative medium for 7 days, and we allowed them to differentiate on poly-L-lysine-coated coverslips for 4 additional days. We kept the *Foxg1* transgene on during the entire procedure. Following *Foxg1* overactivation, we found a pronounced loss of S100 $\beta$ <sup>+</sup> astrocytes ( $-63.89 \pm 9.14\%$ ,  $P < 0.003$ ,  $n = 4,4$ ) as well as a consistent reduction of Gfap<sup>+</sup> cells ( $-37.32 \pm 20.10\%$ ,  $P < 0.002$ ,  $n = 3,3$ ) (Figs 1H,I and S1G,H) (Gfap is an intermediate filament protein, mainly confined to astrocytes of rodent neocortex (Malatesta et al. 2008)). Remarkably, this anti-differentiative effect was specific to the astroglial lineage, as, within the same cultures, the frequency

of Tubb3<sup>+</sup> neurons was almost doubled ( $+90.45 \pm 4.53\%$ ,  $P < 0.03$ ,  $n = 3,3$ ) (Figs 1H,I and S1I). In a second test, astroglial cultures were conversely prepared from *Foxg1*<sup>1-/-</sup> (Hébert and McConnell 2000) mice-derived corticocerebral precursors. In this case, no S100 $\beta$ <sup>+</sup> output change was detected compared with wild type controls (Figs 1J,K and S1K). As in previous in vivo assays, we also evaluated the frequencies of NSCs in both *Foxg1*-GOF and -LOF cultures and used them to normalize the number of S100 $\beta$ <sup>+</sup> and Gfap<sup>+</sup> cells. (Here, NSCs were identified as expressing Sox2 but not an mCherry reporter under the control of the neuronogenic-lineage-specific *Tubulin- $\alpha$ 1* promoter (Fig. 1H,J)). Interestingly, we found that, at day in vitro (DIV) 4, NSCs were augmented by  $89.64 \pm 10.67\%$  ( $P < 0.0001$ ,  $n = 4,4$ ) in *Foxg1*-GOF cultures and decreased by 26.95% in *Foxg1*-LOF cultures (Figs 1L,K and S1F,J). This implicates that the average, NSC-normalized astrocytic output varied by  $-80.96\%$  (S100 $\beta$ <sup>+</sup> cells) and  $-52.41\%$  (Gfap<sup>+</sup> cells) in *Foxg1*-GOF cultures, as well as by  $+32.93\%$  (S100 $\beta$ <sup>+</sup> cells) in *Foxg1*-LOF cultures.

It is possible that what we observed in our assays did not depend on NSC fate choice, but it alternatively reflected an altered kinetic behavior of astrocyte-committed progenitors originating from engineered NSCs. To fix this issue, we repeated the in vitro *Foxg1*-GOF assay adopting 3 ad hoc devices. First, we ran it over a shorter temporal window (4 days for proliferation and 2 days for differentiation). Second, we took advantage of LIF stimulation to unmask early astroglial committed precursors. Third, we engineered both *Foxg1*-GOF and control preparations by lentiviruses harboring an additional IRES-EGFP module under pNes/TetON control, labeling NSCs and their immediate progenies, and we evaluated the Gfap<sup>+</sup>EGFP<sup>+</sup>/EGFP<sup>+</sup> ratio of each experimental preparation, as a more direct index of NSC-to-astroblast transition. Interestingly, we found that this ratio was diminished by  $52.51 \pm 3.61\%$  in *Foxg1*-GOF samples compared with controls ( $P < 4.7 \times 10^{-5}$ ,  $n = 4,4$ ) (Figs 1L,M and S1L), so confirming the negative impact exerted by *Foxg1* on the NSC astrogenic bias.

To secure this interpretation, we scored *Foxg1*-mutant NSCs by a classical clonal assay. Specifically, we made E11.5 corticocerebral precursors *Foxg1*-GOF or -LOF by dedicated lentiviral effectors, we kept them as floating neurospheres for 4 days, we let them attach on poly-D-lysinated coverslips at clonal density, and we evaluated their clonal outputs 3 days later (Fig. 1N). We observed a decrease of neuron-astrocyte-mixed clones in *Foxg1*-GOF assays ( $5.27 \pm 0.94\%$  in mutants vs.  $25.45 \pm 1.24\%$  in controls,  $P < 10^{-5}$ ,  $n = 4,4$ ) and an increase of these clones in -LOF assays ( $32.83 \pm 2.33\%$  in mutants vs.  $24.81 \pm 3.19\%$  in controls,  $P < 0.04$ ,  $n = 4,4$ ). In case of *Foxg1*-GOF assays, we also found a decrease of astrocyte-only clones ( $1.38 \pm 0.48\%$  in mutants vs.  $5.07 \pm 0.75\%$  in controls,  $P < 3.1 \times 10^{-3}$ ,  $n = 4,4$ ) as well as a concomitant increase of neuron-only clones ( $72.55 \pm 1.33\%$  in mutants vs.  $60.56 \pm 2.14\%$  in controls,  $P < 1.6 \times 10^{-3}$ ,  $n = 4,4$ ) (Figs 1O,P and S1M,N). Altogether, these data show that, in addition to stimulating NSC self-renewal, *Foxg1* antagonizes the NSC shift from neuronogenic towards astrogenic fates.

Finally, before investigating specific antiastrogenic mechanisms driven by *Foxg1*, we wondered about their general articulation, cell-autonomous or not cell-autonomous. As *Foxg1*-GOF precursors gave rise to reduced astroglial outputs upon their transplantation into wild type brains (Fig. 1A,E), we expected that cell-autonomous mechanisms should play a likely prevalent role in this context. To corroborate this inference and unveil possible, collateral nonautonomous processes, we repeated the test shown in Figure 1H,I, with some ad hoc modifications. Specifically, we monitored the histogenetic behavior of aliquots of sensor (S)

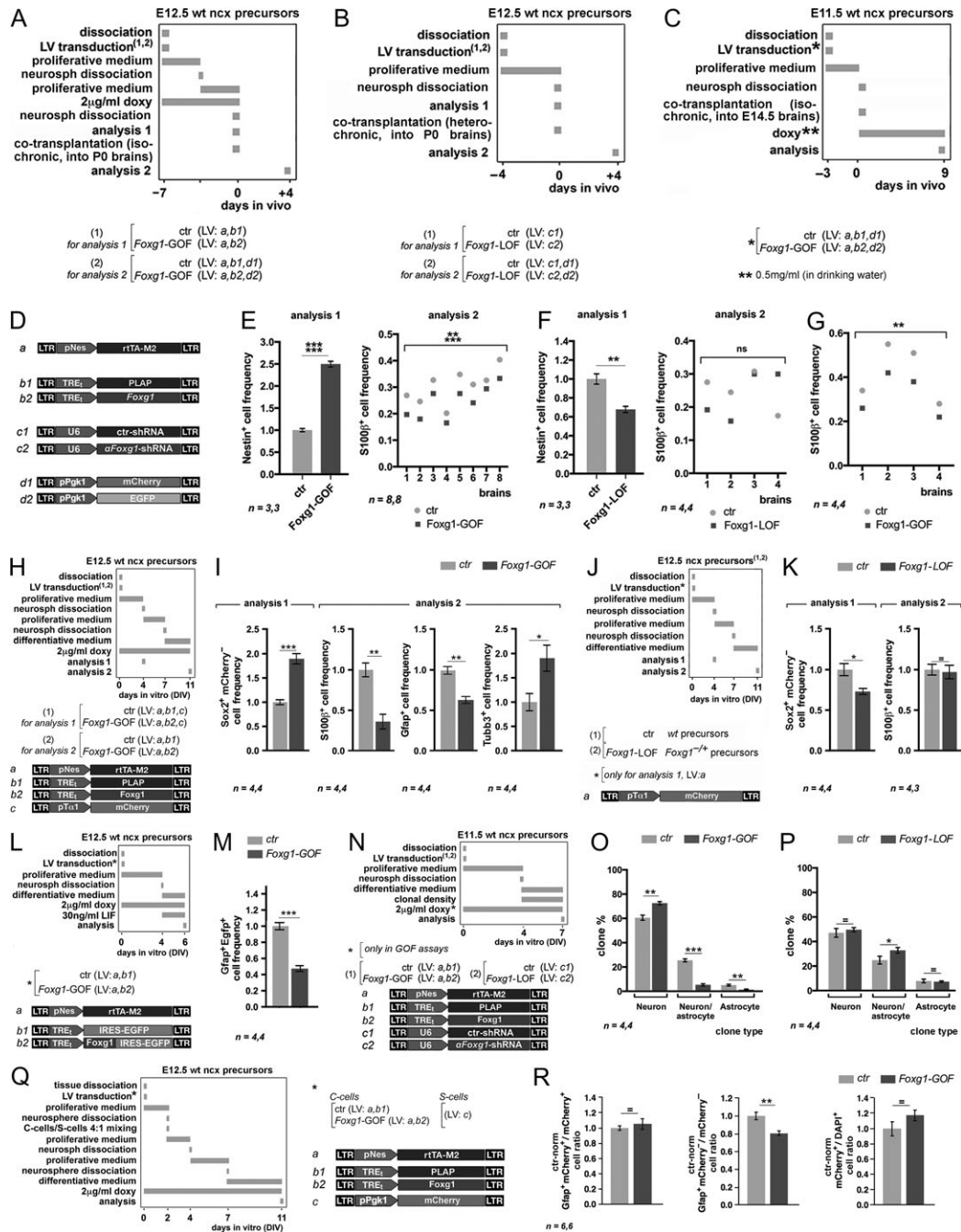


**Figure 1.** Foxg1 antagonizes astrogenic progression of murine corticocerebral stem cells. (A–G) In vivo analysis. (A–C) Experimental strategies, (D) lentiviral vectors employed, and (E–G) results. (E, left) (ctr)-normalized frequencies of Nestin<sup>+</sup> derivatives of E12.5 neocortical (ncx) precursors, acutely infected as in (A, analysis 1) (absolute frequency of Nestin<sup>+</sup> cells in [ctr] samples, 10.38 ± 0.39%). Analysis performed on cells acutely attached on poly-L-lysine-coated coverslips. (E, right) Absolute frequencies of S100β<sup>+</sup> astrocytes, evaluated within the parietal cortex of P4 pups among derivatives of cells engineered as in (A, analysis 2), and cotransplanted as a 1:1 mix into the cortical parietal parenchyma of isochronic P0 pups (average parameter value in [ctr] samples, 30.38 ± 2.24%). (F, left) (ctr)-normalized-frequencies of Nestin<sup>+</sup> derivatives of E12.5 neocortical precursors, acutely infected as in (B, analysis 1) (absolute frequency of Nestin<sup>+</sup> cells in [ctr] samples, 22.45 ± 1.21%). Analysis performed on cells acutely attached on poly-L-lysine-coated coverslips. (F, right) Absolute frequencies of S100β<sup>+</sup> astrocytes, evaluated within the parietal cortex of P4 pups among derivatives of cells engineered as in (B, analysis 2), and cotransplanted as a 1:1 mix into the cortical parietal parenchyma of heterochronic P0 pups (average parameter value in [ctr] samples, 25.04 ± 2.85%). (G) Absolute frequencies of S100β<sup>+</sup> astrocytes, evaluated within the parietal cortex of P4 pups among derivatives of cells engineered as in (C), and cotransplanted as a 1:1 mix into the cortical parietal parenchyma of isochronic E14.5 wild-type embryos (average parameter value in [ctr] samples, 36.27 ± 4.77%). (H–K) In vitro analysis: neural cell frequencies, long protocol. (H, J) Experimental strategy and lentiviral vectors employed for its implementation, and (I, K) results. (I) Results of GOF analysis referred to in (H). Analysis 1: ctr-normalized frequencies of Sox2<sup>+</sup>-mCherry<sup>-</sup> cells at DIV4 (absolute [ctr] frequency, 15.05 ± 0.79%). Cells acutely attached on poly-L-lysine-coated coverslips. Analysis 2 results: ctr-normalized frequencies of S100β<sup>+</sup>, Gfap<sup>+</sup>, and Tubb3<sup>+</sup> cells at DIV11 (absolute [ctr] frequencies, 14.95 ± 1.27%, 21.67 ± 1.03% and 16.85 ± 3.00%, respectively). (K) Results of LOF analysis referred to in (J). Analysis 1: Ctr-normalized frequencies of Sox2<sup>+</sup>-mCherry<sup>-</sup> cells at DIV4 (absolute [ctr] frequency, 14.36 ± 0.10%). Cells acutely attached on poly-L-lysine-coated coverslips. Analysis 2: ctr-normalized frequencies of S100β<sup>+</sup> cells at DIV11 (absolute [ctr] frequency, 25.36 ± 1.70%). (L, M) In vitro analysis: neural cell frequencies, short protocol. (L, M) Experimental strategy, lentiviral vectors employed, and (M) results. Here shown are (ctr)-normalized frequencies of Gfap<sup>+</sup> cells among Egfp<sup>+</sup>-expressing derivatives of

E12.5 wild type pallial precursors, acutely labeled by a constitutively expressed mCherry transgene, following their 1:4 coculture with isochronous conditioner (C) precursors, pre-made GOF for Foxg1 or a control (Fig. 1Q). It turned out that the ratio among Gfap<sup>+</sup>mCherry<sup>+</sup> astrocytes and total mCherry<sup>+</sup> cells was not affected by the “genotype” of the cocultured C-derivative population, while Foxg1 overexpression by C-founders downregulated the fraction of their descendants expressing Gfap ( $-19.44 \pm 2.69\%$ ,  $P < 2.3 \times 10^{-3}$ ,  $n = 6,5$ ) (Fig. 1R). All that confirms that Foxg1 inhibition of astrogenesis largely relies on cell-autonomous mechanisms and suggests that noncell-autonomous processes hardly contribute to it.

### Foxg1 Antagonizes the NSC Astrogenic Progression by Downregulating Key Transcription Factors Channeling NSCs to Astrogenic Fates

We hypothesized that the antiastrogenic activity of Foxg1 could primarily originate from its ability to down-regulate a small set of key transcription factor genes promoting the neuronogenic-versus-astrogenic switch: *Couptf1*, *Sox9*, *Nfia*, and *Zbtb20* (Naka et al. 2008; Kang et al. 2012; Nagao et al. 2016). In fact, Foxg1 is a well known transcriptional inhibitor (Li et al. 1995; Yao et al. 2001). Moreover, as resulting from Jaspar analysis (Mathelier et al. 2014), *Couptf1*, *Sox9*, *Nfia*, and *Zbtb20* loci harbor a number of putative Foxg1-binding sites, among which a few high-score, evolutionarily conserved ones (Fig. S2A–D). We tested this prediction in pre-gliogenic neocortical precursors made Foxg1-GOF by somatic lentiviral transgenesis (Fig. 2A–C; control-norm-[Foxg1-mRNA] =  $4.42 \pm 0.64$ , not shown). As expected, all 4 genes resulted to be downregulated upon Foxg1 overexpression, by  $-41.5 \pm 7.01\%$  ( $P < 0.045$ ,  $n = 4,4$ ),  $-30.98 \pm 5.05\%$  ( $P < 0.046$ ,  $n = 6,6$ ),  $-55.85 \pm 4.73\%$  ( $P < 0.003$ ,  $n = 6,6$ ), and  $-24.30 \pm 9.34\%$  ( $P < 0.038$ ,  $n = 6,6$ ), respectively (Fig. 2D,E). No changes were conversely detectable in Foxg1-knockdown cultures (Fig. 2B,C,F; control-norm-[Foxg1-mRNA] =  $0.65 \pm 0.04$ , not shown), suggesting that gene downregulation observed in Foxg1-GOF preparations did not reflect a dominant-negative effect.

Then, to assess functional relevance of these phenomena to Foxg1 antiastrogenic activity, as a proof-of-principle, we overexpressed *Zbtb20* and *Nfia* in wild type (Fig. S3A–C) and Foxg1-overexpressing precursors and we evaluated the histogenetic outcome of these manipulations by dedicated clonal assays (Fig. 2G). While not fully rescuing the Foxg1-GOF phenotype, the transduction of a constitutively active *Zbtb20* transgene into Foxg1-GOF cultures mitigated the absolute frequency decrease of neuronal-astroglial and astroglial clones evoked by Foxg1 overexpression compared with controls (from  $-25.37\%$  to  $-13.11\%$ ,  $P < 0.009$ ,  $n = 4,4$ , and from  $-7.51\%$  to  $-4.55\%$ ,  $P < 0.021$ ,  $n = 4,4$ , respectively). [Here, control frequencies of neuronal-astroglial and astroglial clones were  $36.23 \pm 2.14\%$  and  $8.89 \pm 1.70\%$ , respectively]. On the other side, *Zbtb20* alone did not significantly alter the frequencies of the different clone types. This suggests that, rather than simply compensating for it, *Zbtb20* transduction partially rescued a key molecular event

mediating Foxg1 impact on NSC fate choice (Figs 2H and S4A). As for *Nfia*, its overexpression in Foxg1-GOF NSCs fully restored the drop of mixed clones caused by Foxg1 upregulation (these clones were as little as  $5.63 \pm 0.48\%$  in Foxg1-GOF cultures compared with  $21.69 \pm 3.53\%$  in controls [ $P < 0.002$ ,  $n = 4,4$ ]), while not affecting the prevalence of these clones if elicited in control NSCs. Moreover, *Nfia* also abolished the slight increase of neuronal clones ( $75.17 \pm 1.73\%$  vs.  $69.49 \pm 2.43\%$ ,  $P < 0.049$ ,  $n = 4,4$ ) as well as the decrease of astroglial ones ( $1.24 \pm 0.46\%$  vs.  $4.62 \pm 0.79\%$ ,  $P < 0.005$ ,  $n = 4,4$ ) caused by Foxg1 overexpression. Remarkably, however, its overactivation in control NSCs almost halved the frequency of neuronal clones ( $40.19 \pm 2.03\%$  vs.  $69.49 \pm 2.43\%$ ,  $P < 0.001$ ,  $n = 4,4$ ) and elicited a massive increase of astroglial ones ( $24.99 \pm 1.17\%$  vs.  $4.62 \pm 0.79\%$ ,  $P < 0.001$ ,  $n = 4,4$ ) (Fig. 2I and S4B). All this indicates that, in addition to rescuing the Foxg1-GOF phenotype, the *Nfia* transgene also overcompensated for it.

Finally, to cast light on molecular mechanisms mediating Foxg1-driven downregulation of *Couptf1*, *Sox9*, *Nfia*, and *Zbtb20*, we profiled chromatin of mid-neuronogenic neocortical precursors, both control and Foxg1-GOF, for Foxg1 recruitment at selected regions of the corresponding loci, by Chromatin Immuno-Precipitation (ChIP)-qPCR (Fig. 2J). Specifically, nine Foxg1-BSs were inspected, 2 for *Couptf1*, 3 for *Zbtb20*, 2 for *Sox9*, and 2 for *Nfia*. These BSs included 4 putative ones selected by Jaspar software (Mathelier et al. 2014), with score index above 14 (<sup>U14</sup>Foxg1-BSs), and shared by mice and humans, as well 5 experimentally verified ones, reported by the NCBI-GEO database (<sup>EXP</sup>Foxg1-BSs) (Fig. S2A–D). In general, all these BSs were specifically enriched in aFoxg1-immunoprecipitates compared with IgG-treated samples (however, this does not apply to *Couptf1*-Foxg1-BS.h1 and *Nfia1*-Foxg1-BS.h1 in control aFoxg1-immuno-precipitates) (Fig. 2K). Interestingly, in case of *Couptf1*, *Sox9* and *Nfia* loci, there was at least one BS significantly over-enriched in Foxg1-GOF compared with control aFoxg1-immunoprecipitates (BSs displaying Foxg1-responsive enrichment included: *Couptf1*-Foxg1-BS.h1 [ $3.83 \pm 0.43\%$  vs.  $1.60 \pm 0.24\%$ ,  $P < 0.005$ ,  $n = 4,3$ ], *Couptf1*-Foxg1-BS.a [ $1.36 \pm 0.15\%$  vs.  $0.88 \pm 0.19\%$ ,  $P < 0.050$ ,  $n = 4,4$ ], *Sox9*-Foxg1-BS.h1 [ $2.02 \pm 0.25\%$  vs.  $1.25 \pm 0.26\%$ ,  $P < 0.025$ ,  $n = 4,3$ ], and *Nfia1*-Foxg1-BS.h1 [ $4.56 \pm 0.47\%$  vs.  $2.66 \pm 0.41\%$ ,  $P < 0.017$ ,  $n = 4,3$ ]) (Fig. 2K). All this suggests that Foxg1 directly transrepresses *Couptf1*, *Sox9*, *Nfia*, and *Zbtb20*, and that such trans-repression may contribute to the decline of *Couptf1*, *Sox9*, and *Nfia* transcripts occurring in Foxg1-GOF precursors.

### Foxg1 Antagonizes Astrogenesis by Directly Transrepressing Astroglial Genes

We hypothesized that Foxg1 inhibition of astrogenesis could be further strengthened by a direct impact of Foxg1 on genes implementing the astroglial differentiation program. To assess this issue, first we investigated the response of selected astroglial genes, *Gfap*, *S100b*, and *Aqp4*, to Foxg1 manipulation. For this purpose, we employed E14.5 corticocerebral precursors engineered

engineered neocortical precursors (absolute [ctr] parameter value,  $19.06 \pm 0.85\%$ ). (N–P) In vitro analysis: clonal assays. (N) Experimental strategy, lentiviral vectors employed, and (O,P) results. Here shown are absolute frequencies of Tubβ3<sup>+</sup>Gfap<sup>+</sup> (neuron-only), Tubβ3<sup>+</sup>Gfap<sup>+</sup> (astrocyte-only), Tubβ3<sup>+</sup>Gfap<sup>+</sup> (neuron-astrocyte-mixed) clones, as evaluated among total clones originating from E11.5 neocortical precursors, infected and processed as in (N). (Q, R) In vitro analysis: cell-autonomous versus noncell-autonomous mechanisms. (Q) Experimental strategy, lentiviral vectors employed, and (R) results. Here, shown are (ctr)-normalized Gfap<sup>+</sup>mCherry<sup>+</sup>/mCherry<sup>+</sup> and Gfap<sup>+</sup>mCherry<sup>-</sup>/mCherry<sup>-</sup> cell number ratios, as well as (ctr)-normalized mCherry<sup>+</sup> cell frequencies, as evaluated in DIV11 cultures originating from of E12.5 neocortical (ncx) precursors, acutely infected, and processed as in (Q). (absolute [ctr] parameter values,  $56.50 \pm 1.70\%$ ,  $41.57 \pm 1.78\%$ , and  $16.12 \pm 1.49\%$ , respectively). Error bar = s.e.m.  $n$  is the number of biological replicates (i.e., independently transduced cell samples, or—case (E, right), (F, right), and (G)—cotransplanted brains). P-value calculated by t-test (one-tail, unpaired, or—case (E, right), (F, right) and (G)—one-tail, paired).

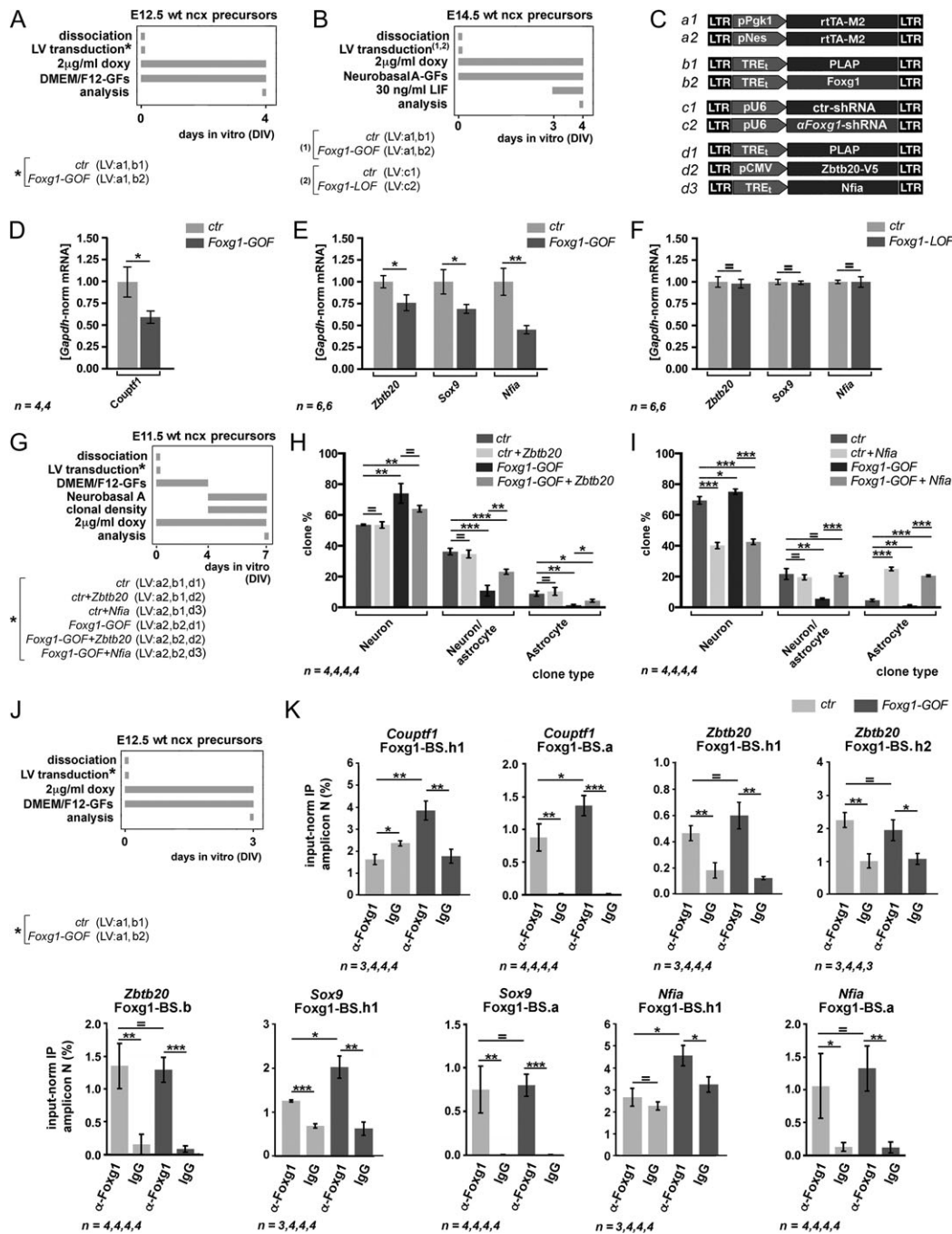


**Figure 2.** *Foxg1* downregulates key effectors directing NSCs to astrogenic fates. (A–F) Impact of *Foxg1* manipulation on *Couptf1*, *Zbtb20*, *Sox9*, and *Nfia* mRNA levels in late embryonic corticocerebral precursors. (A, B) Experimental protocols, (C) lentiviral vectors employed, and (D–F) results ((D) referring to (A), (E, F) to (B)). Data double-normalized, against endogenous *Gapdh*-mRNA and (ctr) values. (G–I) Functional relevance of *Zbtb20* and *Nfia* misregulation to *Foxg1* antiastrogenic activity. This was tested by antagonizing *Foxg1*-driven expression changes of these effectors and interrogating the engineered cultures by clonal analysis, similar to Figure 1N,O. (G) Experimental protocol, (C) lentiviral vectors employed, and (H, I) results. (J, K) Chromatin Immunoprecipitation-PCR (ChIP-PCR) quantification of *Foxg1*-enrichment at putative *Foxg1* binding sites within *Couptf1*, *Zbtb20*, *Sox9*, and *Nfia* loci (named as in Fig. S2A–D): (J) experimental protocol and (K) results. Data normalized against input chromatin. Error bar = s.e.m. *n* is the number of biological replicates (i.e., independently transduced cell samples). *P*-value calculated by t-test (one-tail, unpaired).

for TetON-controlled *Foxg1* overexpression, kept in the presence of growth factors and terminally pulsed by LIF (Fig. 3A). As expected, we found that *Gfap*-, *S100b*-, and *Aqp4*-mRNA levels were significantly decreased, by  $-49.92 \pm 13.25\%$  ( $P < 0.03$ ,  $n = 6,6$ ),  $-46.79 \pm 16.91\%$  ( $P < 0.03$ ,  $n = 5,5$ ), and  $-43.98 \pm 14.70\%$  ( $P < 0.03$ ,  $n = 5,5$ ), respectively (Fig. 3B, left). No statistically significant

changes of these mRNAs were observed in a specular *Foxg1*-LOF assay (Fig. 3B, right), so ruling out any dominant negative effects.

Next, to cast light on mechanisms mediating *Foxg1*-dependent repression of these genes, we selected a set of putative *Foxg1*-binding sites (BSs) within *Gfap*, *S100b*, and *Aqp4* promoters (2 for *Gfap*, 3 for *S100b* and 2 for *Aqp4*), by Jasp software

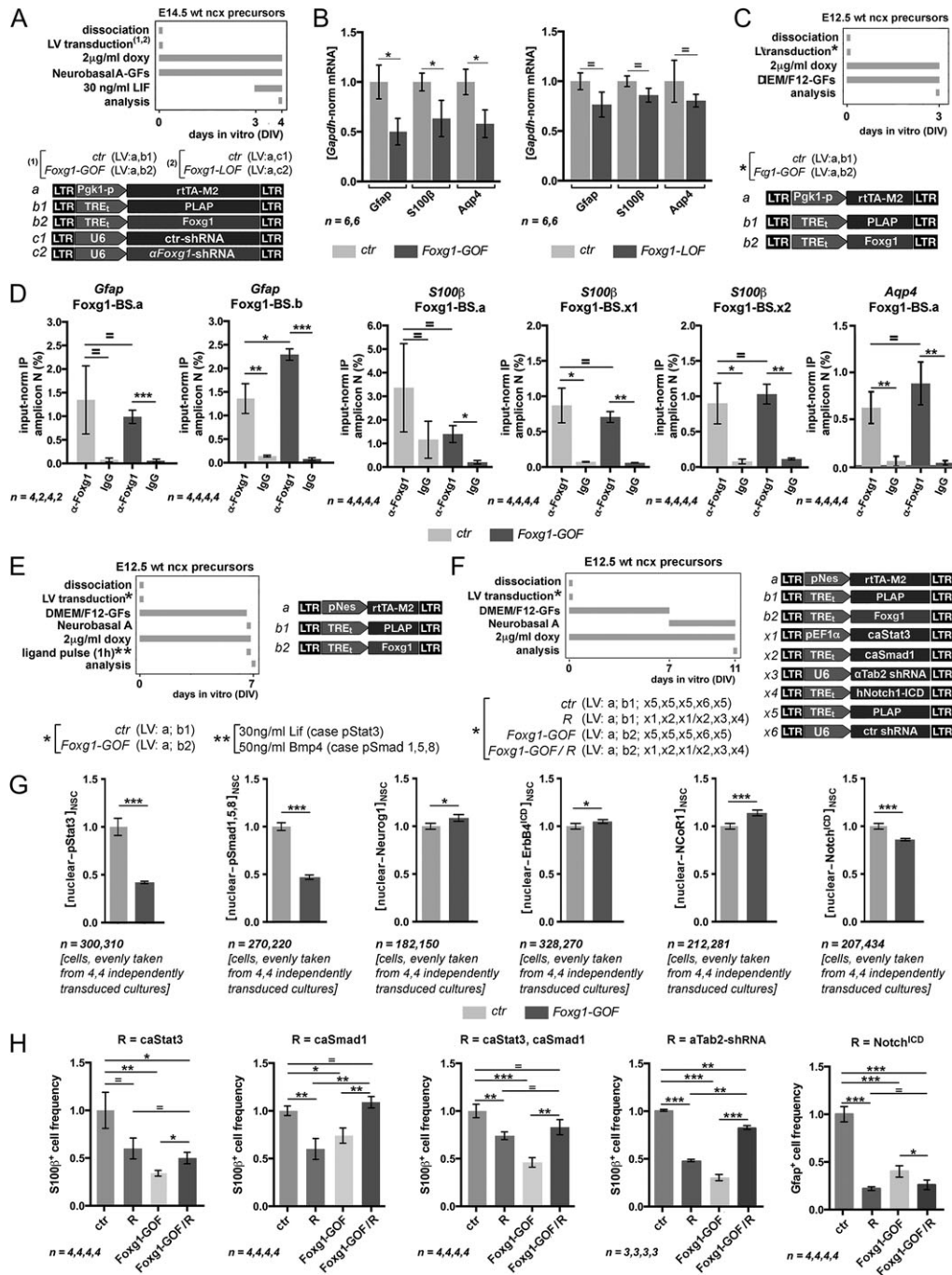


**Figure 3.** Foxg1 represses astroglial-lineage active genes. (A, B) Regulation of astroglial *Gfap*, *S100b* and *Aqp4* genes by Foxg1: (A) experimental strategy, lentiviral vectors employed, and (B) results. Data double-normalized, against endogenous *Gapdh*-mRNA and (ctr) values. (C, D) Assaying direct regulation mechanisms: Chromatin ImmunoPrecipitation-PCR (qChIP-PCR) quantification of Foxg1-enrichment at putative Foxg1 binding sites within *Gfap*, *S100b* and *Aqp4* loci (named as in Fig. S2E-G); (C) experimental strategy, lentiviral vectors employed, and (D) results. Data normalized, against input chromatin. (E-J) Assaying indirect regulation mechanisms. (E, G) Modulation of nuclear pStat3, pSmad1,5,8, ErbB4<sup>ICD</sup>, NCoR1, Notch1<sup>ICD</sup> protein levels in Nestin<sup>+</sup>, E12.5+DIV7 neural stem cells (NSCs), overexpressing Foxg1, evaluation by quantitative immunofluorescence. (E) Experimental protocol, lentiviral vectors employed, and (G) results. Data normalized against (ctr). (F, H) Functional relevance of pStat3, pSmad1,5,8, ErbB4<sup>ICD</sup>, NCoR1, and Notch1<sup>ICD</sup> misregulation to Foxg1 antiastrogenic activity, assessed by counteracting Foxg1-driven changes of these effectors and evaluating the resulting S100b<sup>+</sup> cell frequency. Constitutively active Stat3 and Smad1 (caStat3 and caSmad1) were overexpressed one by one or combined; functional relevance of ErbB4<sup>ICD</sup> and NCoR1 was investigated by dampening their essential Tab2 cofactor. (F) Experimental protocol, lentiviral vectors employed, and (H) results. Data normalized against (ctr); absolute frequencies of S100b<sup>+</sup> cells: 11.84 ± 2.30% (ctr<sub>pStat3</sub>), 8.58 ± 0.43% (ctr<sub>pSmad1,5,8</sub>), 8.87 ± 0.62% (ctr<sub>pStat3-pSmad1,5,8</sub>), 21.36 ± 5.27% (ctr<sub>Tab2</sub>); absolute frequencies of Gfap<sup>+</sup> cells: 37.59 ± 3.14% (ctr<sub>Notch1-ICD</sub>). Data normalized against (ctr). Error bar = s.e.m. n is the number of biological replicates. These are: (B, D, H) independently transduced neural cultures; (G) single cells, randomly and evenly picked from 4,4 independently transduced neural cultures. P-values calculated by t-test (one-tail, unpaired).

(Mathelier et al. 2014) (Fig. S2E–G). Then, we monitored the actual recruitment of *Foxg1* to these sites, both in control and *Foxg1*-GOF cells, by ChIP-qPCR. To this aim, we employed chromatin extracted from derivatives of E12.5 corticocerebral precursors, processed as in Figure 3C. We found that the chromatin enrichment elicited by a*Foxg1* ranged from  $0.63 \pm 0.17\%$  (*Aqp4*\_Foxg1-BS.a,  $n = 4,4$ ) to  $3.36 \pm 1.87\%$  (*S100b*\_Foxg1-BS.a,  $n = 4,4$ ) in control samples, well above the background ChIP signal given by control IgG. Moreover, such enrichment did not generally change in *Foxg1*-GOF samples, suggesting that *Foxg1* binds to these sites with high affinity. In the only case of *Gfap*\_Foxg1-BS.b, this enrichment—about  $1.36 \pm 0.32\%$  in controls—arose up to  $2.29 \pm 0.12\%$  upon *Foxg1* overexpression ( $P < 1.7 \times 10^{-3}$ ,  $n = 4,4$ ) (Fig. 3D). This means that this interaction could contribute to differential regulation of *Gfap* in *Foxg1*-GOF samples.

### Foxg1 Antagonizes Astrogenesis Via a Pleiotropic Impact on Key Pathways Tuning Astroglial Genes

In addition to its direct effect on astroglial genes, we hypothesized that *Foxg1* might further dampen their activity indirectly, by impacting transactive modulators of their transcription. In particular, we focused our attention on 4 key pathways involved in fundamental control of astroglial gene transcription: IL6/Jak2/Stat1,3; Bmp/Smad1,5,8; Nrg1/ErbB4<sup>ICD</sup>-NCoR; Dll1/Notch1<sup>ICD</sup>. For these pathways, we measured nuclear levels of their ultimate nuclear effectors (modulating gene transcription) within *Foxg1*-GOF, Nestin<sup>+</sup> NSCs. We also evaluated nuclear NSC levels of a key antagonist of the IL6/Jak2/Stat1,3 pathway, Neurog1. We acutely engineered E12.5 corticocerebral precursors, making them to overexpress *Foxg1* in the neurostem compartment. We kept these precursors in culture under growth factors for 7 days, and we finally coimmunoprofiled them for Nestin and the 6 effectors in order, each evaluated by quantitative immunofluorescence (qIF): p[Tyr<sup>705</sup>]Stat3, p[Ser<sup>463/465</sup>]Smad1,5,8, Neurog1, ErbB4<sup>ICD</sup>, NCoR1, and Notch1<sup>ICD</sup> (Fig. 3E). We found that p[Tyr<sup>705</sup>]Stat3, p[Ser<sup>463/465</sup>]Smad1,5,8, and Notch1<sup>ICD</sup> were downregulated, by  $-58.28 \pm 1.99\%$  ( $P < 2.5 \times 10^{-10}$ ,  $n = 300\ 310$ ),  $-52.91 \pm 2.34\%$  ( $P < 5.8 \times 10^{-23}$ ,  $n = 270\ 220$ ), and  $-13.78 \pm 1.20\%$  ( $P < 2.7 \times 10^{-7}$ ,  $n = 207,404$ ), respectively. ErbB4<sup>ICD</sup> was unaffected. Conversely, Neurog1 and NCoR1 were slightly, albeit significantly upregulated, by  $+8.75 \pm 3.56\%$  ( $P < 0.032$ ,  $n = 182\ 150$ ) and  $+14.18 \pm 2.83\%$  ( $P < 0.0002$ ,  $n = 212\ 281$ ), respectively (Figs 3G and S4C–H).

To address the relevance of such changes to astrogenesis inhibition, we functionally counteracted them by transducing E12.5 neocortical precursors, made acutely *Foxg1*-GOF, with pre-validated (Fig. S3D–G), “rescuing” Xi lentiviruses. We kept engineered cells as proliferating neurospheres for 7 days under growth factors. We allowed them to differentiate for 4 more days. Finally, we evaluated their S100b<sup>+</sup> astroglial output (Fig. 3F). We found that constitutively active Stat3 (caStat3) (Hillion et al. 2008) lessened the astroglial deficit elicited by *Foxg1* overexpression, however only to a limited extent (normalized against controls, this deficit moved from  $-66.46 \pm 3.15\%$  to  $-49.70 \pm 6.29\%$ ,  $P < 0.03$ ,  $n = 4,4$ ). Conversely, constitutively active Smad1 (Fuentelba et al. 2007) (caSmad1), alone or in combination with caStat3, fully restored the normal astroglial output. In a similar way, functional NCoR1 inhibition, via knockdown of its necessary Tab2 cofactor (Sardi et al. 2006), considerably reduced the *Foxg1*-dependent astrogenic deficit (Figs 3H and S6A–D). Remarkably, in all these cases the delivery of the “rescuing agent” to control cultures did not upregulate astrogenesis rates (caStat3 and caSmad1 reduced the output of these cultures (Fig. 3H), possibly because of

premature shrinkage of their neurostem compartment (Fig. S5A)). All this suggests that each of these agents did not simply mask the astrogenic deficit elicited by *Foxg1* overexpression, via compensatory mechanisms independent from *Foxg1* regulation. It rather indicates that they abolished molecular abnormalities which specifically mediate the impact of *Foxg1* overexpression on astrogenesis. Last, NSC transduction of a constitutively active Notch<sup>ICD</sup> transgene (Cassady et al. 2014) failed to rescue the hypoastrogenic *Foxg1*-GOF phenotype. Moreover, it reduced the Gfap<sup>+</sup> astroglial output of both control and *Foxg1*-GOF cultures, from  $100 \pm 8.35\%$  to  $21.64 \pm 2.48\%$  (control-normalized frequencies,  $P < 0.001$ ,  $n = 4,4$ ), and from  $40.28 \pm 5.63\%$  to  $26.34 \pm 4.71\%$  (control-normalized frequencies,  $P < 0.001$ ,  $n = 4,4$ ), respectively (Figs 3H and S6E). This phenomenon was unexpected. It likely reflected the defective capability of derivatives of Notch<sup>ICD</sup>-overexpressing NSCs to respond to astrogenic cytokines and activate the mature astroglial marker Gfap (Fig. S5B).

Next, we investigated basic mechanisms leading to pStat3 and pSmad1,5,8 deficits. We evaluated the impact of *Foxg1* manipulations on key players implicated in the corresponding signaling machineries (Fig. 4A). As for the IL6/Jak2/Stat1,3 axis, we found a significant downregulation of *Gp130*-, *Jak2*-, and *Stat3*-mRNAs (*Gp130*:  $-24.51 \pm 6.53\%$ ,  $P < 0.05$ ,  $n = 6,6$ ; *Jak2*:  $-54.33 \pm 6.52\%$ ,  $P < 0.0002$ ,  $n = 6,6$ ; *Stat3*:  $-32.26 \pm 8.88\%$ ,  $P < 0.03$ ,  $n = 6,6$ ) and no changes for *Il6Ra*-mRNA in *Foxg1*-GOF cultures (Fig. 4B). *Jak2*- and *Stat3*-mRNA were conversely upregulated in *Foxg1*-LOF cultures (*Jak2*:  $+13.32 \pm 3.80\%$ ,  $P < 0.02$ ,  $n = 6,6$ ; *Stat3*:  $+10.59 \pm 2.44\%$ ,  $P < 0.02$ ,  $n = 6,6$ ), whereas *Gp130*- and *Il6Ra*-RNA were unaffected (Fig. 4C). Concerning the Bmp/Smad1,5,8 pathway, *BmpRII*-mRNA was downregulated in *Foxg1*-GOF samples ( $-29.59 \pm 11.44\%$ ,  $P < 0.03$ ,  $n = 6,6$ ) (Fig. 4B) and unaffected in *Foxg1*-LOF ones (Fig. 4C). *Bmp4* was not affected at all. Last, NCoR1-mRNA levels, implicated in the balance between Notch<sup>ICD</sup> and ErbB4<sup>ICD</sup>-mediated signaling, did not show any significant change either in *Foxg1*-GOF and -LOF cultures (Fig. 4B,C). Finally, as a proof-of-principle, to assess relevance of the changes described above to the *Foxg1*-GOF astroglial phenotype, we counteracted the *Jak2*-mRNA decline peculiar to *Foxg1*-GOF neocortical precursors by a lentiviral expressor encoding for the constitutively active, JAK2<sup>V617F</sup> mutant kinase (Vainchenker 2005), and we evaluated the impact of this manipulation on Gfap<sup>+</sup> cell frequency (Fig. 4D). Interestingly, the introduction of a JAK2<sup>V617F</sup> transgene in *Foxg1*-GOF cultures mitigated the decline of Gfap<sup>+</sup> cells caused by *Foxg1* overexpression, which moved from  $-43.13 \pm 4.02\%$  to  $-30.26 \pm 2.84\%$  (control-normalized frequencies,  $P < 0.020$ ,  $n = 4,4$ ). The frequency of these cells was conversely unaffected, when JAK2<sup>V617F</sup> was delivered to controls (Figs 4E and S6F). All this suggests that the downregulation of *Jak2* (and, possibly, other *Foxg1*-sensitive, IL6/Jak2/Stat1,3- and Bmp/Smad1,5,8-signaling mediators reported above) may contribute to *Foxg1* inhibition of astroglial genes expression.

### Foxg1 Impairs Transactivating Abilities of the pStat3–pSmad1,5,8 Complex

It was previously shown that *Foxg1* chelates Smad1 and Smad4 (Rodriguez et al. 2001). Therefore, we wondered if it may antagonize astrogenesis, by impairing intrinsic transactivating abilities of these Bmp signaling effectors. To address this issue, we acutely engineered E12.5 neocortical precursors with 2 transgenes, encoding for constitutively active Stat3 (caStat3) and Smad1 (caSmad1), driven by a constitutive promoter (*Pgk1*-p). To sense the activity of the resulting caStat3-caSmad1 complex

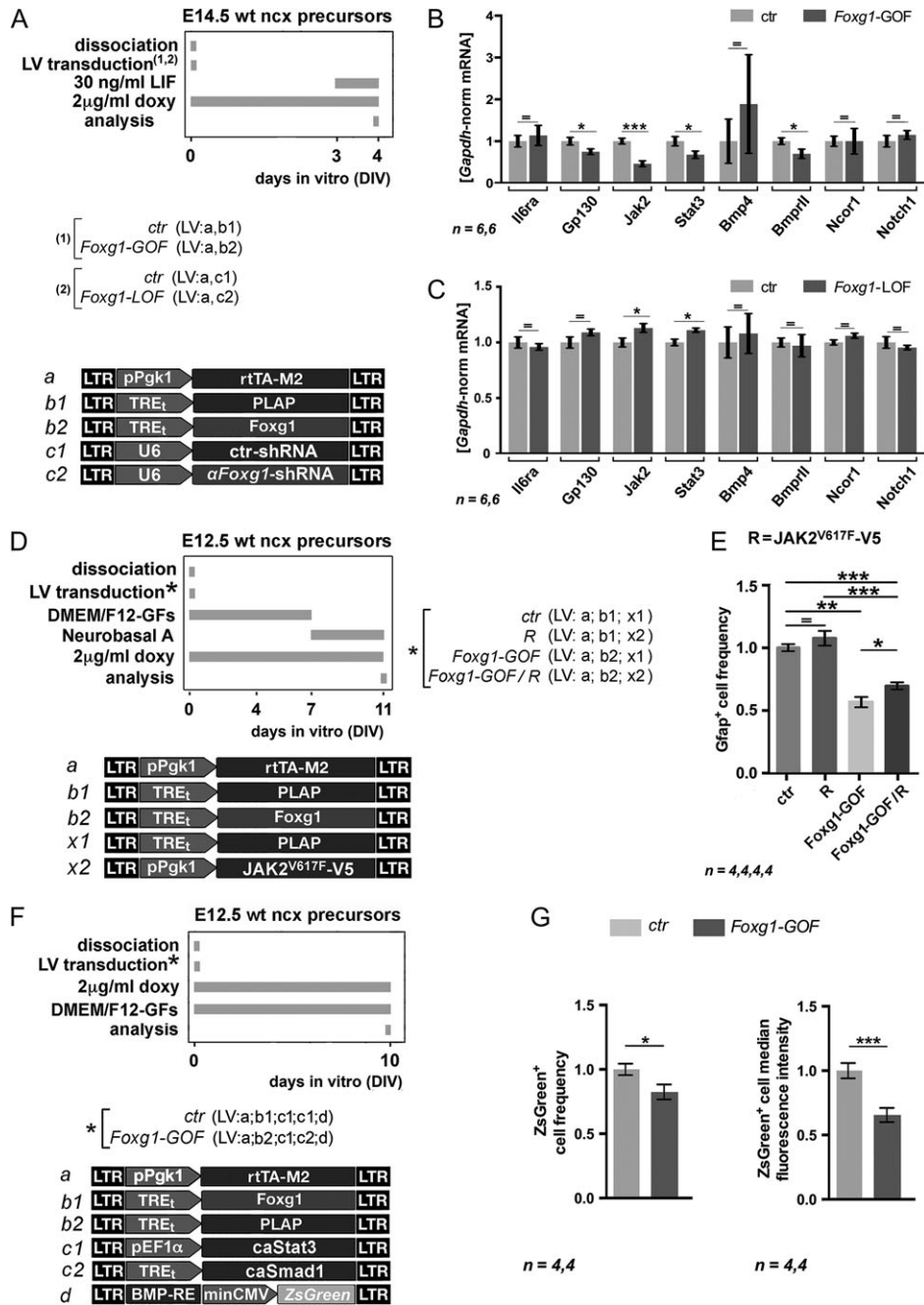


**Figure 4.** Molecular details of Foxg1 impact on different astrogenic pathways. (A–C) Consequences of Foxg1 manipulation on mRNA levels of *IL6Ra*, *Gp130*, *Jak2*, *Stat3*, *Bmp4*, *BmprII*, *NCoR1*. (A) Experimental protocol and lentiviral vectors employed, (B, C) results. Data double-normalized, against endogenous *Gapdh*-mRNA and (ctr) values. (D, E) Functional relevance of *Jak2* misregulation to Foxg1 antiastrogenic activity. This was assessed by counteracting Foxg1-driven change of *Jak2*-mRNA and evaluating the resulting S100b<sup>+</sup> cell frequency: (D) experimental protocol and lentiviral vectors employed, (E) results. Data normalized against (ctr); absolute frequency of S100b<sup>+</sup> cells in (ctr) samples:  $28.70 \pm 0.81\%$ . (F, G) Foxg1 impact on transactivating abilities of BMP/Jak-Stat pathways effectors. This was assessed by expressing caStat3 and caSmad1 in E12.5 neocortical precursor cultures and evaluating their ability to transactivate a lentivector-delivered, randomly integrating fluorescent reporter gene, associated to Bmp responsive elements (BMP-RE), upon Foxg1 overexpression. (F) Experimental protocol, lentiviral vectors employed, and (G) (ctr)-normalized results. Analysis by cytofluorometry. Absolute (ctr) frequency of ZsGreen<sup>+</sup> cells:  $78.50 \pm 5.33\%$ . Error bar = s.e.m. n is the number of biological replicates. P-values calculated by t-test (one-tail, unpaired).

in a way independent of possible local epigenetic effects of Foxg1 on astroglial gene chromatin, we employed a synthetic Bmp-signaling sensor (*BmpRE-ZsGreen*), delivered via a randomly integrating lentivector. To so-engineered neural cells, we concomitantly delivered aFoxg1-expressing lentivirus or a control. We kept these cells for 10 days in proliferative

conditions and, lastly, we profiled them for EGFP fluorescence by cytofluorometry (Fig. 4F). We found that both the frequency of ZsGreen<sup>+</sup> cells and the median fluorescence intensity of ZsGreen<sup>+</sup> cells were reduced in Foxg1-GOF samples, by  $38.38 \pm 6.63\%$  (control-normalized value,  $P < 0.05$ ,  $n = 4,4$ ), and  $26.88 \pm 2.78\%$  (control-normalized value,  $P < 0.001$ ,  $n = 4,4$ ), respectively

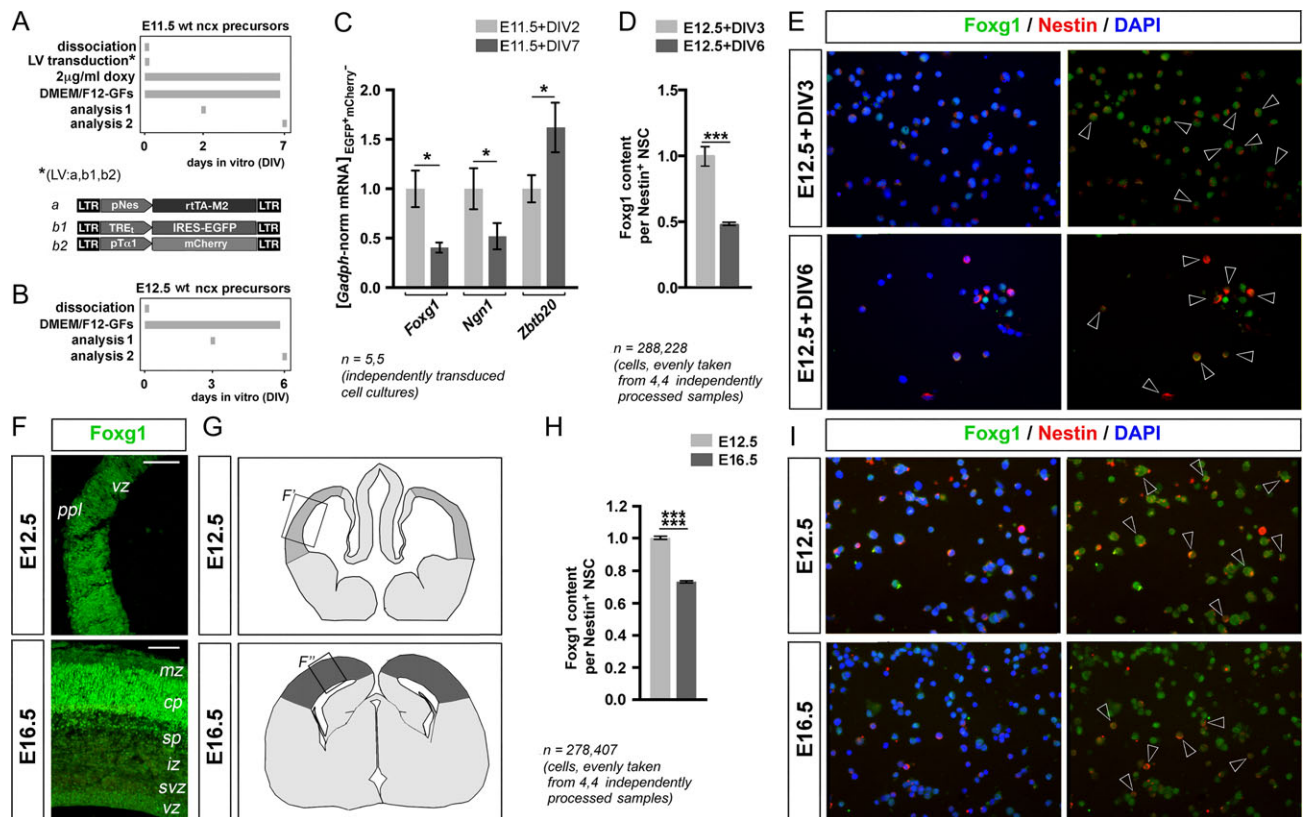


**Figure 5.** Neocortical stem cell *Foxg1* levels decrease prior to the neocortical astrogenic wave. (A, C) *Foxg1*-mRNA levels in *in vitro* aging neural stem cells, labeled by lentiviral tracers, identified as pNes-Egfp<sup>+</sup>/pTa1-mCherry<sup>-</sup> and purified by FACsorting. In (A) experimental protocol, in (C) results. *Ngn1* and *Zbtb20* are shown as controls. Data double-normalized, against endogenous *Gapdh*-mRNA and “E11.5+DIV2” values. (B, D, E) *Foxg1*-protein levels in *in vitro* aging neural stem cells, recognized as Nestin<sup>+</sup> cells and scored by quantitative immunofluorescence. In (B) experimental protocol, in (D) results and in (E) example pictures. Data normalized against E12.5 average value. Empty arrowheads in (E) point to Nestin<sup>+</sup> elements. (F) *In vivo* distribution of *Foxg1* protein in neocortical periventricular layers of E12.5 and E16.5 embryos. (G, H) *Foxg1*-protein levels in acutely dissociated, Nestin<sup>+</sup> neural stem cells taken from E12.5 and E16.5 neocortices, scored by quantitative immunofluorescence. In (G) results, in (H) localization of sampled cells, in (I) primary data examples. Empty arrowheads in (I) point to Nestin<sup>+</sup> elements. Error bar = s.e.m. *n* is the number of biological replicates. These are: (C) independently transduced neural cultures, or (D, H) single cells, randomly and evenly picked from 4,4 independently transduced neural cultures (D) and 4,4 acutely dissociated neocortices (H). *P*-values calculated by *t*-test (one-tail, unpaired).

(Fig. 4G). Conversely, in a parallel control assay where the *BmpRE-ZsGreen* *Bmp*-signaling sensor was replaced by a *pPgl1-mCherry* transgene, no *mCherry* expression decline was detectable in *Foxg1*-GOF samples (not shown). These results suggest that *Foxg1* may dampen the intrinsic, pSmad1/4 transactivating power.

### ***Foxg1* NSC Expression Levels Progressively Decline Before the Perinatal Astrogenic Burst**

We wondered if *Foxg1* antiastrogenic activity might be instrumental in the proper temporal progression of astrogenesis. Specifically, we hypothesized that high *Foxg1* levels in early NSCs could refrain them from differentiating to astroblasts, while lower levels peculiar to later NSCs could be permissive to such differentiation. To address this issue, we measured *Foxg1*-mRNA and -protein levels within pallial stem cells of different ages.

In a first assay, we employed derivatives of E11.5 precursors, cultured in propoliferative medium for 2 up to 7 days. From these cultures we FACsorted samples of NSCs (identified as pNes-EGFP<sup>+</sup>/pTa1-mCherry<sup>-</sup>, upon lentiviral transduction of these reporters) at DIV2 and DIV7, approximately corresponding to *in vivo* E13.5 and E18.5, respectively. We analyzed their RNA and we found a significant decrease of *Foxg1*-mRNA level

in DIV7 compared with DIV2 samples ( $-59.47 \pm 5.11\%$ ,  $P < 0.01$ ,  $n = 5,5$ ). Here, as controls, we also measured expression of *Zbtb20* and *Neurog1*, 2 genes active in NSCs according to opposite temporal progressions (Hirabayashi et al. 2009; Ohtsuka et al. 2011). As expected, *Zbtb20* and *Neurog1* were increased and decreased, respectively, in more aged samples (Fig. 5A,B). In a second assay, we evaluated *Foxg1* protein level in DIV2 and DIV6 Nestin<sup>+</sup> NSC derivatives of E12.5 acutely dissociated neocortices, by double aNestin-a*Foxg1* qIF. Compared with DIV2 samples, *Foxg1* level was diminished by  $52.55 \pm 1.47\%$  at DIV6 ( $P < 3.6 \times 10^{-10}$ ,  $n = 288,229$ ) (Fig. 5C,D), confirming that a robust *Foxg1* expression decline occurs in neocortical stem cells concomitantly with the neuronogenic-to-astrogenic transition.

To corroborate these findings, we compared *in vivo* *Foxg1* expression at late versus early neuronogenic stages of neocortical development. As expected, we found that periventricular *Foxg1* levels overtly declined at E16.5 with respect to E12.5 (Fig. 5F). Consistently, qIF profiling of acutely dissociated neocortices showed that a  $-27.19 \pm 1.2\%$  *Foxg1* decline ( $P < 8.18 \times 10^{-40}$ ,  $n = 407,278$ ) specifically occurred in E16.5 Nestin<sup>+</sup> NSCs compared with E12.5 ones (Fig. 5G,H). In other words the *Foxg1* decline preceded the transition from neuronogenesis to astrogenesis, suggesting it could be instrumental in arousal of the latter.

## Foxg1 Antiastrogenic Activity is Conserved in Human Pallial Precursors

To assess if FOXG1 antagonizes astrogenesis progression in humans like in rodents, we run an ad hoc GOF assay in late pallial precursors derived from a legal, human PCW10 abortion, pre-expanded in vitro over about 150 days. At the beginning of the procedure (DIV0), we transduced these precursors with 2 lentiviruses, expressing the rtTA<sup>M2</sup> transactivator under the constitutive *Pgk1* promoter and *Foxg1* (or a control) under the rtTA<sup>M2</sup>/doxycycline-responsive TREt promoter (Fig. 6A). We kept the engineered cells for 7 days in proliferation medium and 7 more days in differentiation medium. We exposed them to 9 ng/ml doxycyclin from DIV0 to DIV11 (so eliciting a final expression gain about 4, not shown) and we immunoprofiled their derivatives at DIV15 for S100b (which is mainly confined to cells expressing the pan-astrocytic marker AldoC in these cultures; not shown). It turned out that S100b<sup>+</sup> astrocyte frequency was reduced by  $-51.29 \pm 8.05\%$  in *Foxg1*-GOF samples compared with controls ( $P < 0.006$ ,  $n = 4,4$ ) (Figs 6A and S7A). To get a closer insight into FOXG1 role in human NSC fate choice, we run an additional GOF assay, differing from the previous 1 in 3 aspects. We restricted *Foxg1* overexpression to the NSC compartment, under the control of the *pNes* promoter; we shortened the differentiation phase of the procedure by 4 days; we exposed the engineered cells to a terminal, 24 h pulse of LIF. Then, we evaluated the frequency of cells expressing GFAP (specifically detectable in astroglial, but also neurostem human cells (Malatesta et al. 2008)) as a proxy of the NSC astrogenic bias (Fig. 6B). Immunoprofiling of these cultures at DIV10 showed that such frequency was reduced by  $-27.66 \pm 5.41\%$  in *Foxg1*-GOF samples compared with controls ( $P < 0.003$ ,  $n = 4,4$ ) (Figs 6B and S7B). All this supports the hypothesis that *Foxg1* may antagonize the NSC astrogenic progression in humans like in rodents.

Next, to corroborate these results and rule out that they originated from a dominant negative effect, we interrogated a sister preparation of the PCW10 neocortical precursors referred to above, pre-expanded in vitro over about 120 days, by a NSC-restricted FOXG1-LOF approach (Figs 6C and S7C). For this purpose, we transduced such precursors by a lentiviral mix encoding for *pNes*-driven expression of miR.aFoxg1.1690 (this is an RNAi effector decreasing FOXG1-mRNA levels by about 42% upon constitutive, *Pgk1p*-driven expression in mixed neural cultures; data not shown). Then, we kept transduced cells 7 days in proliferative medium and 3 more days in a differentiative medium, terminally supplemented by LIF. Finally, we immunoprofiled cells for neurostem/astroglial markers. Frequency of Egfp<sup>+</sup>GFAP<sup>+</sup> astrocytes was unaffected. Conversely, normalized against controls, Egfp<sup>+</sup>GFAP<sup>+</sup> NSCs were reduced by  $-26.97 \pm 7.82\%$  ( $P < 0.025$ ,  $n = 3,3$ ). All this points to a robust increase of the NSC-normalized GFAP<sup>+</sup> astroglial output (normalized against controls,  $+58.59 \pm 3.83\%$ ,  $P < 0.003$ ,  $n = 3,3$ ) (Fig. 6C). It further suggests that the negative FOXG1 impact on NSC astrogenic progression emerging from overexpression assays is a genuine GOF phenotype.

Last, to assess a possible conservation of mechanisms mediating *Foxg1* impact on astrogenesis progression, we downregulated FOXG1 in human, PCW10+DIV120 neocortical precursors by a constitutively expressed RNAi effector (*aFoxg1*-shRNA) and monitored the impact of this manipulation on human orthologs of murine mediators of this activity (Fig. 6D). We found that, upon a  $-22.19 \pm 3.73\%$  decline of FOXG1-mRNA ( $P < 0.049$ ,  $n = 3,3$ ), ZBTB20-mRNA was upregulated by  $+26.48 \pm 2.72\%$  ( $P < 0.005$ ,  $n = 3,3$ ), and

COUPTF1, SOX9 and NFIA were unaffected. Moreover, mRNAs of *Egfp* and *ZsGreen* reporters, driven by pStat1,3- and Bmp-responsive elements (REs) and codelivered to neural cells by dedicated lentivectors with a *Pgk1p*-driven *mCherry* normalizer, were also robustly upregulated, by  $+252.55 \pm 105.72\%$  ( $P < 0.025$ ,  $n = 3,2$ ) and  $+168.81 \pm 71.90\%$  ( $P < 0.050$ ,  $n = 3,3$ ), respectively (Fig. 6D). All that suggest that key molecular mechanisms mediating *Foxg1* control of astrogenesis are shared by placental mammals.

## Discussion

In this study we showed that *Foxg1* overexpression within murine neocortical stem cells antagonizes the generation of astrocytes, in vivo as well as in vitro, while stimulating NSC self-renewal and promoting neuronogenesis (Fig. 1). We discovered that *Foxg1* antiastrogenic activity can originate from 4 concurrent mechanisms. *Foxg1* transrepresses key transcription factor genes promoting the NSC-to-astrocyte progenitor progression (Fig. 2). It also directly transrepresses astroglial genes, that is, genes implementing the astroglial differentiation program (Fig. 3A–D). Next, it tunes multiple key pathways controlling astroglial gene transcription, unbalancing nuclear concentration of their ultimate effectors (pStat3, pSmad1,5,8, NCoR1, Notch<sup>ICD</sup>) and so further dampening astroglial gene expression (Figs 3E–H and 4A–E). Last, it jeopardizes transactivating abilities of one of these effectors, the pStat3–pSmad1,5,8 complex (Fig. 4F,G). Moreover, we found that *Foxg1* levels within neocortical NSCs progressively decline prior to the neuronogenic-to-gliogenic transition (Fig. 5), suggesting an involvement of *Foxg1* in fine temporal tuning of astrogenesis rates. Finally, we provided a proof-of-principle that a similar antiastrogenic activity is played by *Foxg1* in human neocortical precursors (Fig. 6), pointing to such activity as an evolutionarily conserved trait.

Interestingly, a robust *Foxg1*-dependent inhibition of astrogenesis was observed in vivo, upon a variety of functional assays (Fig. 1A–G). In particular, a shrinkage of the astroglial output occurred only when *Foxg1* was upregulated (Fig. 1E,G and 6A–C), ruling out any artifactual dominant negative effect. Furthermore, after normalization of such output against the starting size of the NSC compartment (Fig. 1E,F and 6A–C), *Foxg1* capability to inhibit astrogenesis emerged upon both gain- and loss-of-function approaches, suggesting that this process is sensitive to even subtle changes of *Foxg1* levels around baseline. Noticeably, these observations were performed upon transplantation of neural precursors premanipulated in vitro by lentiviral transgenesis, an approach allowing for stable and accurate control of gene expression levels.

Next, the astrogenesis decline evoked by *Foxg1* overexpression in NSCs was not simply due to a general differentiation deficit of neocortical precursors. In fact, it was associated to a pronounced, absolute increase of neuronogenesis (Fig. 1H,I). As emerging from clonal assays (Fig. 1N–P), this did reflect a net, consistent shift in the NSC histogenetic choice. This means that channeling NSCs towards neuronal rather than glial fates is a genuine, key role exerted by *Foxg1* in normal development.

Last, an antiastrogenic activity was observed when NSC-restricted *Foxg1* overexpression was switched on in vivo, in a late-neuronogenic, isochronic environment (Fig. 1C,G). Moreover, clone founder cells showed an altered astrogenic bias following *Foxg1* manipulation during the neuronogenic phase (Fig. 1N–P). Not least, *Foxg1* NSC levels (both mRNA and protein) turned out to progressively decline, while moving from early neuronogenic stages to subsequent gliogenic phases (Fig. 5). All this suggests

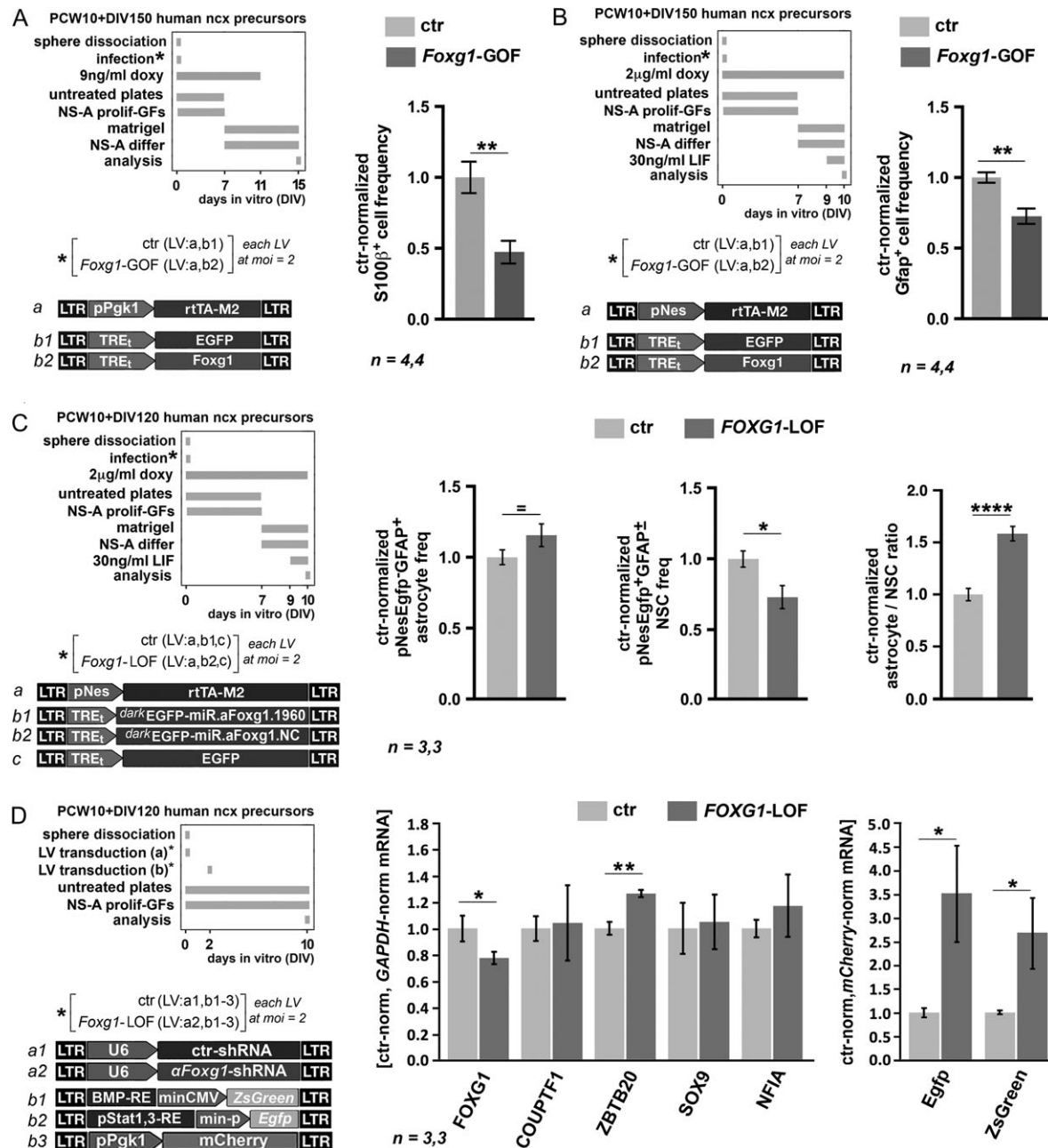


**Figure 6.** Foxg1 inhibits progression of human pallial precursors towards astrogenesis. (A–C) Impact of FOXG1 modulation on astrogenic outputs of engineered human neocortical precursors: temporal articulation of the histogenetic assays, lentiviral vectors employed, and results. The tests were run on late human neocortical precursors, derived from PCW10 abortions and pre-expanded in vitro over 150 (A, B) or 120 (C) days. Astrocytic outputs were evaluated upon (A) constitutive (pPgk1-rtTA<sup>M2</sup>-driven) or (B) NSC-restricted (pNestin-rtTA<sup>M2</sup>-driven) Foxg1-GOF manipulations, as well as upon (C) constitutive FOXG1 knockdown via a U6 promoter-driven, aFoxg1-shRNA transgene (FOXG1-LOF samples). Shown are control-normalized frequencies of S100b<sup>+</sup> (A) and GFAP<sup>+</sup> cells (B), pNesEgfp<sup>+</sup>GFAP<sup>+</sup> astrocytes and pNesEgfp<sup>+</sup>GFAP<sup>+</sup> NSCs (C), as well as control-normalized pNesEgfp<sup>+</sup>GFAP<sup>+</sup> / pNesEgfp<sup>+</sup>GFAP<sup>+</sup> cell ratios (C). Absolute control frequencies of S100b<sup>+</sup> cells (A), GFAP<sup>+</sup> cells (B), pNesEgfp<sup>+</sup>GFAP<sup>+</sup> astrocytes and pNesEgfp<sup>+</sup>GFAP<sup>+</sup> NSCs (C), 24.70 ± 4.00%, 12.62 ± 0.46%, 23.38 ± 1.45% and 44.16 ± 2.54%, respectively. (D) Modulation of putative genes and pathways mediating the impact of FOXG1 downregulation on astrogenesis: protocols, lentiviruses employed and results. Shown are control/GAPDH-double-normalized, FOXG1, COUPTF1, ZBTB20, SOX9, and NFIA mRNA levels, as well as control/mCherry-double-normalized, Egfp (pStat1,3-RE-Egfp) and ZsGreen (BMP-RE-ZsGreen) mRNA levels. Error bar = s.e.m. n is the number of biological replicates, that is, independently transduced neural cultures. P-values calculated by t-test (one-tail, unpaired).

that a progressive decline of Foxg1 levels is among key factors dictating age-dependent, NSC developmental choices (Ohtsuka et al. 2011; Okamoto et al. 2016).

As for cellular articulation of Foxg1 activity, it has to be emphasized that astrogenesis inhibition was detectable upon NSC-restricted Foxg1 overexpression (Figs 1A,C,D,H,N and 6B),

by scoring progenies of engineered neural precursors transplanted in wild type brains (Fig. 1E,G) or allowed to differentiate in vitro (Figs 1I,O and 6B). It is known that, despite the relevance of environmental signals to the progression of early pallial precursors towards gliogenesis (Morrow et al. 2001), such progression can largely occur in a clone-autonomous way (Qian



B). The latter, at odds with *Foxg1*-dependent upregulation of the canonical *Neurog1* inhibitor, *Hes1* (Cau et al. 2000; Brancaccio et al. 2010; Chiola et al. 2019), was perhaps promoted by *Foxg1* via *Pax6* (Blader 2004; Manuel et al. 2010). Regardless of mechanisms unbalancing their levels, both pStat1 and *Neurog1* are known to compete for limited p300 and pSmad1 cofactors available, to form an active trimer which transactivates astroglial or neuronal genes, respectively (Nakashima 1999; Sun et al. 2001). In this way, in the presence of reduced pSmad1 levels, even a moderate decline of the pStat1/*Neurog1* ratio may have a truly disruptive effect on astroglial genes activation.

In a similar way, even the subtle changes of nuclear NCoR1 and Notch<sup>ICD</sup> evoked by *Foxg1* (Fig. 3G) might significantly concur to defective astrogenic performances of *Foxg1*-GOF NSCs. In fact, both these factors compete for the same RBPJk bridge (Kao et al. 1998), mediating their interaction with astroglial genes (Ge et al. 2002; Hermanson et al. 2002). In this way, the increase of the NCoR1/Notch<sup>ICD</sup> ratio occurring in *Foxg1*-GOF NSC nuclei ( $(114.18/86.22-1) \times 100\% = +32.42\%$ , Fig. 3G) might severely unbalance this competition, so resulting in prevailing inhibitory, RBPJk-mediated inputs to astroglial promoters. To note, the moderate upregulation of nuclear NCoR1 occurring in *Foxg1*-GOF samples (Fig. 3G), not due to NCoR1 gene transactivation (Fig. 4A,B), could reflect the decline of the IL6/Jak2/Stat3 cascade, instrumental in its nucleus-to-cytoplasm translocation (Sardi et al. 2006). As for Notch<sup>ICD</sup>, we largely ignore mechanisms underlying its dynamics. Moreover, the apparently negative impact of its overexpression on the astroglial output (Fig. 3G and S5B) deserves further investigations.

Last, *Foxg1* regulation of astrogenesis is not peculiar to rodents. In fact, we found that similar phenomena can be detected when *Foxg1* expression levels are manipulated in human pallial precursors. In this respect, it has been shown that an abnormal FOXG1 copy number results in severe neurological pathologies, such as a variant of Rett syndrome, linked to FOXG1 haploinsufficiency (Guerrini and Parrini 2012), and a variant of West syndrome, associated to FOXG1 duplication (Pontrelli et al. 2014). It is tempting to speculate that an alteration of astrogenesis profiles may take place in these patients and concur to their neurological symptoms.

In synthesis, we have found that *Foxg1* antagonizes astrogenesis in the developing rodent neocortex. We have disentangled a large body of molecular mechanisms mediating this activity. We have shown that *Foxg1* may contribute to proper temporal articulation of the NSC histogenetic bias. Finally, we have provided a proof-of-principle that *Foxg1* regulation of astrogenesis can be an evolutionary conserved trait, shared by different mammals.

### Authors' Contributions

C.F. dissected *Foxg1* functions in murine neocortical precursors, analyzed the results and cowrote the article, M.S. contributed to dissect *Foxg1* functions in murine and human neocortical precursors, G.L. and N.C. contributed to assays with murine precursors, G.C. performed initial experiments with human precursors, A.V. took care of cytofluorometry, L.P.J. and S.P. provided human neocortical precursors, A.M. designed the study, analyzed the results, and wrote the article.

### Supplementary Material

Supplementary material is available at *Cerebral Cortex* online.

### Funding

Telethon Italy (Grant GGP13034 to A.M.) and SISSA (intramurary funding to A.M.).

### Notes

We thank Nika Blecich who contributed to early setup of in vitro histogenetic assays. We are grateful to Marco Bestagno and Nicoletta Caronni for technical assistance in FACsorting procedures, as well as to Alberto Tommasini for supporting us with analytic cytofluorimetric assays. *Conflict of Interest:* The authors declare no competing interests.

### References

- Barnabé-Heider F, Wasylnka JA, Fernandes KJL, Porsche C, Sendtner M, Kaplan DR, Miller FD. 2005. Evidence that embryonic neurons regulate the onset of cortical gliogenesis via cardiotrophin-1. *Neuron*. 48:253–265.
- Blader P. 2004. Conserved and acquired features of neurogenin1 regulation. *Development*. 131:5627–5637.
- Brancaccio M, Pivetta C, Granzotto M, Filippis C, Mallamaci A. 2010. *Emx2* and *Foxg1* inhibit gliogenesis and promote neurogenesis. *Stem Cells*. 28:1206–1218.
- Cassady JP, D'Alessio AC, Sarkar S, Dani VS, Fan ZP, Ganz K, Roessler R, Sur M, Young RA, Jaenisch R. 2014. Direct lineage conversion of adult mouse liver cells and B lymphocytes to neural stem cells. *Stem Cell Reports*. 3:948–956.
- Cau E, Gradwohl G, Casarosa S, Kageyama R, Guillemot F. 2000. *Hes* genes regulate sequential stages of neurogenesis in the olfactory epithelium. *Development*. 127:2323–2332.
- Chiola S, Do MD, Centrone L, Mallamaci A. 2019. *Foxg1* overexpression in neocortical pyramids stimulates dendrite elongation via *Hes1* and pCreb1 upregulation. *Cereb Cortex*. 29(3):1006–1019.
- Costa MR, Bucholz O, Schroeder T, Götz M. 2009. Late origin of glia-restricted progenitors in the developing mouse cerebral cortex. *Cereb Cortex*. 19:i135–i143.
- Deloulme JC, Raponi E, Gentil BJ, Bertacchi N, Marks A, Labourdette G, Baudier J. 2004. Nuclear expression of S100B in oligodendrocyte progenitor cells correlates with differentiation toward the oligodendroglial lineage and modulates oligodendrocytes maturation. *Mol Cell Neurosci*. 27:453–465.
- Derouet D, Rousseau F, Alfonsi F, Froger J, Hermann J, Barbier F, Perret D, Diveu C, Guillet C, Preisser L, et al. 2004. Neuropoietin, a new IL-6-related cytokine signaling through the ciliary neurotrophic factor receptor. *Proc Natl Acad Sci USA*. 101:4827–4832.
- Falcone C, Filippis C, Granzotto M, Mallamaci A. 2015. *Emx2* expression levels in NSCs modulate astrogenesis rates by regulating *Egfr* and *Fgf9*. *Glia*. 63:412–422.
- Fuentealba LC, Eivers E, Ikeda A, Hurtado C, Kuroda H, Pera EM, De Robertis EM. 2007. Integrating patterning signals: Wnt/GSK3 regulates the duration of the BMP/Smad1 signal. *Cell*. 131:980–993.
- Ge W, Martinowich K, Wu X, He F, Miyamoto A, Fan G, Weinmaster G, Sun YE. 2002. Notch signaling promotes astroglialogenesis via direct CSL-mediated glial gene activation. *J Neurosci Res*. 69:848–860.
- Ge W-P, Miyawaki A, Gage FH, Jan YN, Jan LY. 2012. Local generation of glia is a major astrocyte source in postnatal cortex. *Nature*. 484:376–380.

- Gorski JA, Talley T, Qiu M, Puelles L, Rubenstein JLR, Jones KR. 2002. Cortical excitatory neurons and glia, but not GABAergic neurons, are produced in the Emx1-expressing lineage. *J Neurosci.* 22:6309–6314.
- Guerrini R, Parrini E. 2012. Epilepsy in Rett syndrome, and CDKL5 - and FOXG1 -gene-related encephalopathies: MECP2-CDKL5-FOXG1-related encephalopathies. *Epilepsia.* 53:2067–2078.
- Hall MD, Murray CA, Valdez MJ, Perantoni AO. 2017. Mesoderm-specific Stat3 deletion affects expression of Sox9 yielding Sox9-dependent phenotypes. *PLoS Genet.* 13:e1006610.
- Hanashima C, Fernandes M, Hebert JM, Fishell G. 2007. The role of Foxg1 and dorsal midline signaling in the generation of Cajal-Retzius subtypes. *J Neurosci.* 27:11103–11111.
- He F, Ge W, Martinowich K, Becker-Catania S, Coskun V, Zhu W, Wu H, Castro D, Guillemot F, Fan G, et al. 2005. A positive autoregulatory loop of Jak-STAT signaling controls the onset of astroglialogenesis. *Nat Neurosci.* 8:616–625.
- Hermanson O, Jepsen K, Rosenfeld MG. 2002. N-CoR controls differentiation of neural stem cells into astrocytes. *Nature.* 419:934–939.
- Hillion J, Dhara S, Sumter TF, Mukherjee M, Di Cello F, Belton A, Turkson J, Jaganathan S, Cheng L, Ye Z, et al. 2008. The high-mobility group A1a/signal transducer and activator of transcription-3 axis: an achilles heel for hematopoietic malignancies? *Cancer Res.* 68:10121–10127.
- Hirabayashi Y, Suzuki N, Tsuboi M, Endo TA, Toyoda T, Shinga J, Koseki H, Vidal M, Gotoh Y. 2009. Polycomb limits the neurogenic competence of neural precursor cells to promote astrogenic fate transition. *Neuron.* 63:600–613.
- Hébert JM, McConnell SK. 2000. Targeting of cre to the Foxg1 (BF-1) locus mediates loxP recombination in the telencephalon and other developing head structures. *Dev Biol.* 222:296–306.
- Jeselsohn R, Cornwell M, Pun M, Buchwalter G, Nguyen M, Bango C, Huang Y, Kuang Y, Paweletz C, Fu X, et al. 2017. Embryonic transcription factor SOX9 drives breast cancer endocrine resistance. *Proc Natl Acad Sci USA.* 114:E4482–E4491.
- Kamakura S, Oishi K, Yoshimatsu T, Nakafuku M, Masuyama N, Gotoh Y. 2004. Hes binding to STAT3 mediates crosstalk between Notch and JAK-STAT signalling. *Nat Cell Biol.* 6:547–554.
- Kang P, Lee HK, Glasgow SM, Finley M, Donti T, Gaber ZB, Graham BH, Foster AE, Novitsch BG, Gronostajski RM, et al. 2012. Sox9 and NFIA coordinate a transcriptional regulatory cascade during the initiation of gliogenesis. *Neuron.* 74:79–94.
- Kanski R, van Strien ME, van Tijn P, Hol EM. 2014. A star is born: new insights into the mechanism of astrogenesis. *Cell Mol Life Sci.* 71:433–447.
- Kao HY, Ordentlich P, Koyano-Nakagawa N, Tang Z, Downes M, Kintner CR, Evans RM, Kadesch T. 1998. A histone deacetylase corepressor complex regulates the Notch signal transduction pathway. *Genes Dev.* 12:2269–2277.
- Li J, Chang HW, Lai E, Parker EJ, Vogt PK. 1995. The oncogene qin codes for a transcriptional repressor. *Cancer Res.* 55:5540–5544.
- Magavi S, Friedmann D, Banks G, Stolfi A, Lois C. 2012. Coincident generation of pyramidal neurons and protoplasmic astrocytes in neocortical columns. *J Neurosci.* 32:4762–4772.
- Malatesta P, Appolloni I, Calzolari F. 2008. Radial glia and neural stem cells. *Cell Tissue Res.* 331:165–178.
- Mallamaci A. 2013. Developmental control of cortico-cerebral astrogenesis. *Int J Dev Biol.* 57:689–706.
- Manuel M, Martynoga B, Yu T, West JD, Mason JO, Price DJ. 2010. The transcription factor Foxg1 regulates the competence of telencephalic cells to adopt subpallial fates in mice. *Development.* 137:487–497.
- Mariani J, Coppola G, Zhang P, Abyzov A, Provini L, Tomasini L, Amenduni M, Szekely A, Palejev D, Wilson M, et al. 2015. FOXG1-dependent dysregulation of GABA/glutamate neuron differentiation in autism spectrum disorders. *Cell.* 162:375–390.
- Mathelier A, Zhao X, Zhang AW, Parcy F, Worsley-Hunt R, Arenillas DJ, Buchman S, Chen C, Chou A, Ienasescu H, et al. 2014. JASPAR 2014: an extensively expanded and updated open-access database of transcription factor binding profiles. *Nucleic Acids Res.* 42:D142–D147.
- Miller FD, Gauthier AS. 2007. Timing is everything: making neurons versus glia in the developing cortex. *Neuron.* 54:357–369.
- Miyoshi G, Fishell G. 2012. Dynamic FoxG1 expression coordinates the integration of multipolar pyramidal neuron precursors into the cortical plate. *Neuron.* 74:1045–1058.
- Morrow T, Song MR, Ghosh A. 2001. Sequential specification of neurons and glia by developmentally regulated extracellular factors. *Development.* 128:3585–3594.
- Muzio L, Mallamaci A. 2005. Foxg1 confines Cajal-Retzius neurogenesis and hippocampal morphogenesis to the dorsomedial pallium. *J Neurosci.* 25:4435–4441.
- Nagao M, Ogata T, Sawada Y, Gotoh Y. 2016. Zbtb20 promotes astrocytogenesis during neocortical development. *Nat Commun.* 7:11102.
- Naka H, Nakamura S, Shimazaki T, Okano H. 2008. Requirement for COUP-TFI and II in the temporal specification of neural stem cells in CNS development. *Nat Neurosci.* 11(9):1014–1023.
- Nakashima K. 1999. Synergistic signaling in fetal brain by STAT3-Smad1 complex bridged by p300. *Science.* 284:479–482.
- Namihira M, Kohyama J, Semi K, Sanosaka T, Deneen B, Taga T, Nakashima K. 2009. Committed neuronal precursors confer astrocytic potential on residual neural precursor cells. *Dev Cell.* 16:245–255.
- Nielsen JV, Blom JB, Noraberg J, Jensen NA. 2010. Zbtb20-induced CA1 pyramidal neuron development and area enlargement in the cerebral midline cortex of mice. *Cereb Cortex.* 20:1904–1914.
- Nielsen JV, Nielsen FH, Ismail R, Noraberg J, Jensen NA. 2007. Hippocampus-like corticogenesis induced by two isoforms of the BTB-zinc finger gene Zbtb20 in mice. *Development.* 134:1133–1140.
- Ohtsuka T, Shimojo H, Matsunaga M, Watanabe N, Kometani K, Minato N, Kageyama R. 2011. Gene expression profiling of neural stem cells and identification of regulators of neural differentiation during cortical development. *Stem Cells.* 29:1817–1828.
- Okamoto M, Miyata T, Konno D, Ueda HR, Kasukawa T, Hashimoto M, Matsuzaki F, Kawaguchi A. 2016. Cell-cycle-independent transitions in temporal identity of mammalian neural progenitor cells. *Nat Commun.* 7:11349.
- Okano H, Temple S. 2009. Cell types to order: temporal specification of CNS stem cells. *Curr Opin Neurobiol.* 19:112–119.
- Patriarchi T, Amabile S, Frullanti E, Landucci E, Lo Rizzo C, Ariani F, Costa M, Olimpico F, W Hell J, M Vaccarino F, et al. 2016. Imbalance of excitatory/inhibitory synaptic protein expression in iPSC-derived neurons from FOXG1(+/-) patients and in foxg1(+/-) mice. *Eur J Hum Genet.* 24:871–880.
- Pluchino S, Gritti A, Blezer E, Amadio S, Brambilla E, Borsellino G, Cossetti C, Del Carro U, Comi G, 't Hart B, et al. 2009.

- Human neural stem cells ameliorate autoimmune encephalomyelitis in non-human primates. *Ann Neurol.* 66:343–354.
- Pontrelli G, Cappelletti S, Claps D, Sirloto P, Ciocca L, Petrocchi S, Terracciano A, Serino D, Fusco L, Vigevano F, et al. 2014. Epilepsy in patients with duplications of chromosome 14 Harboring FOXP1. *Pediatr Neurol.* 50:530–535.
- Qian X, Shen Q, Goderie SK, He W, Capela A, Davis AA, Temple S. 2000. Timing of CNS cell generation: a programmed sequence of neuron and glial cell production from isolated murine cortical stem cells. *Neuron.* 28:69–80.
- Raponi E, Agenes F, Delphin C, Assard N, Baudier J, Legraverend C, Deloulme J-C. 2007. S100B expression defines a state in which GFAP-expressing cells lose their neural stem cell potential and acquire a more mature developmental stage. *Glia.* 55:165–177.
- Rodriguez C, Huang LJ-S, Son JK, McKee A, Xiao Z, Lodish HF. 2001. Functional cloning of the proto-oncogene brain factor-1 (BF-1) as a smad-binding antagonist of transforming growth factor- $\beta$  signaling. *J Biol Chem.* 276:30224–30230.
- Sardi SP, Murtie J, Koirala S, Patten BA, Corfas G. 2006. Presenilin-dependent ErbB4 nuclear signaling regulates the timing of astrogenesis in the developing brain. *Cell.* 127:185–197.
- Schlessinger J, Lemmon MA. 2006. Nuclear signaling by receptor tyrosine kinases: the first robin of spring. *Cell.* 127:45–48.
- Sloan SA, Barres BA. 2014. Mechanisms of astrocyte development and their contributions to neurodevelopmental disorders. *Curr Opin Neurobiol.* 27:75–81.
- Sun Y, Nadal-Vicens M, Misono S, Lin MZ, Zubiaga A, Hua X, Fan G, Greenberg ME. 2001. Neurogenin promotes neurogenesis and inhibits glial differentiation by independent mechanisms. *Cell.* 104:365–376.
- Takouda J, Katada S, Nakashima K. 2017. Emerging mechanisms underlying astrogenesis in the developing mammalian brain. *Proc Jpn Acad Ser B Phys Biol Sci.* 93:386–398.
- Toma K, Kumamoto T, Hanashima C. 2014. The timing of upper-layer neurogenesis is conferred by sequential derepression and negative feedback from deep-layer neurons. *J Neurosci.* 34:13259–13276.
- Tonchev AB, Tuoc TC, Rosenthal EH, Studer M, Stoykova A. 2016. Zbtb20 modulates the sequential generation of neuronal layers in developing cortex. *Mol Brain.* 9(1):65.
- Tsai H-H, Li H, Fuentealba LC, Molofsky AV, Taveira-Marques R, Zhuang H, Tenney A, Murnen AT, Fancy SPJ, Merkle F, et al. 2012. Regional astrocyte allocation regulates CNS synaptogenesis and repair. *Science.* 337:358–362.
- Vainchenker W. 2005. A unique activating mutation in JAK2 (V617F) is at the origin of polycythemia vera and allows a new classification of myeloproliferative diseases. *Hematology.* 2005:195–200.
- Yao J, Lai E, Stifani S. 2001. The winged-helix protein brain factor 1 interacts with groucho and hes proteins to repress transcription. *Mol Cell Biol.* 21:1962–1972.